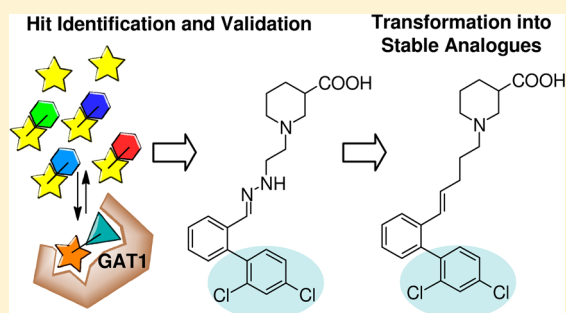


Focused Pseudostatic Hydrazone Libraries Screened by Mass Spectrometry Binding Assay: Optimizing Affinities toward γ -Aminobutyric Acid Transporter 1Miriam Sindelar, Toni A. Lutz, Marilena Petrera,[†] and Klaus T. Wanner*

Center for Drug Research, Department of Pharmacy, Ludwig Maximilians University at Munich, Butenandtstrasse 9-13, D-81377 Munich, Germany

S Supporting Information

ABSTRACT: Mass spectrometric (MS) binding assays, a powerful tool to determine affinities of single drug candidates toward chosen targets, were recently demonstrated to be suitable for the screening of compound libraries generated with reactions of dynamic combinatorial chemistry when rendering libraries pseudostatic. Screening of small hydrazone libraries targeting γ -aminobutyric acid transporter 1 (GAT1), the most abundant γ -aminobutyric acid (GABA) transporter in the central nervous system, revealed two nipecotic acid derived binders with submicromolar affinities. Starting from the biphenyl carrying hit as lead structure, the objective of the present study was to discover novel high affinity GAT1 binders by screening of biphenyl focused pseudostatic hydrazone libraries formed from hydrazine **10** and 36 biphenylcarbaldehydes **11c–al**. Hydrazone **12z** that carried a 2',4'-dichlorobiphenyl residue was found to be the most potent binder with low nanomolar affinity ($pK_i = 8.094 \pm 0.098$). When stable carba analogues of representative hydrazones were synthesized and evaluated, the best binder **13z** was again displaying the 2',4'-dichlorobiphenyl moiety ($pK_i = 6.930 \pm 0.021$).



INTRODUCTION

γ -Aminobutyric acid (GABA, **1**, Chart 1) is the most abundant inhibitory neurotransmitter in the central nervous system (CNS).^{1–3} A reduced GABAergic neurotransmission, in consequence an imbalance in the neurotransmitter equilibrium, is associated with neurological disorders, e.g., schizophrenia,⁴ Parkinson's disease,⁵ epilepsy,⁶ Alzheimer's disease,⁷ neuropathic pain,⁸ Huntington's disease,⁹ depression,^{10–12} panic,^{10,12} and mania.^{10,12}

To restore the neurotransmitter equilibrium, GABAergic neurotransmission can be enhanced by CNS-active drugs targeting GABA receptors, metabolic enzymes, or GABA transport proteins (GATs). The last targets are membrane bound proteins encoded by genes assigned to the solute carrier 6 (SLC6) family¹³ and mediate the transport of GABA across cell membranes utilizing a co-transport of sodium and chloride ions as energy supply.

Four different subtypes named mGAT1, mGAT2, mGAT3, and mGAT4 when cloned from murine brain cells are known. For other species, the nomenclature for GATs differs, e.g., for the human GATs, the declaration is given by the human genome organization (HUGO) resulting in GAT1, BGT1, GAT2, and GAT3 as corresponding transport proteins.¹⁴ mGAT1 and mGAT4 are the most abundant GABA transporters in the CNS, from which mGAT1 is mainly responsible for the neuronal reuptake of GABA and mGAT4 is predominantly located in cell membranes of glial cells.¹⁵ In contrast, the expression of mGAT2 and mGAT3 in the brain is

very limited. That excludes a significant role in termination of GABA neurotransmission for these proteins for which high densities have been reported in liver and kidney.¹⁶

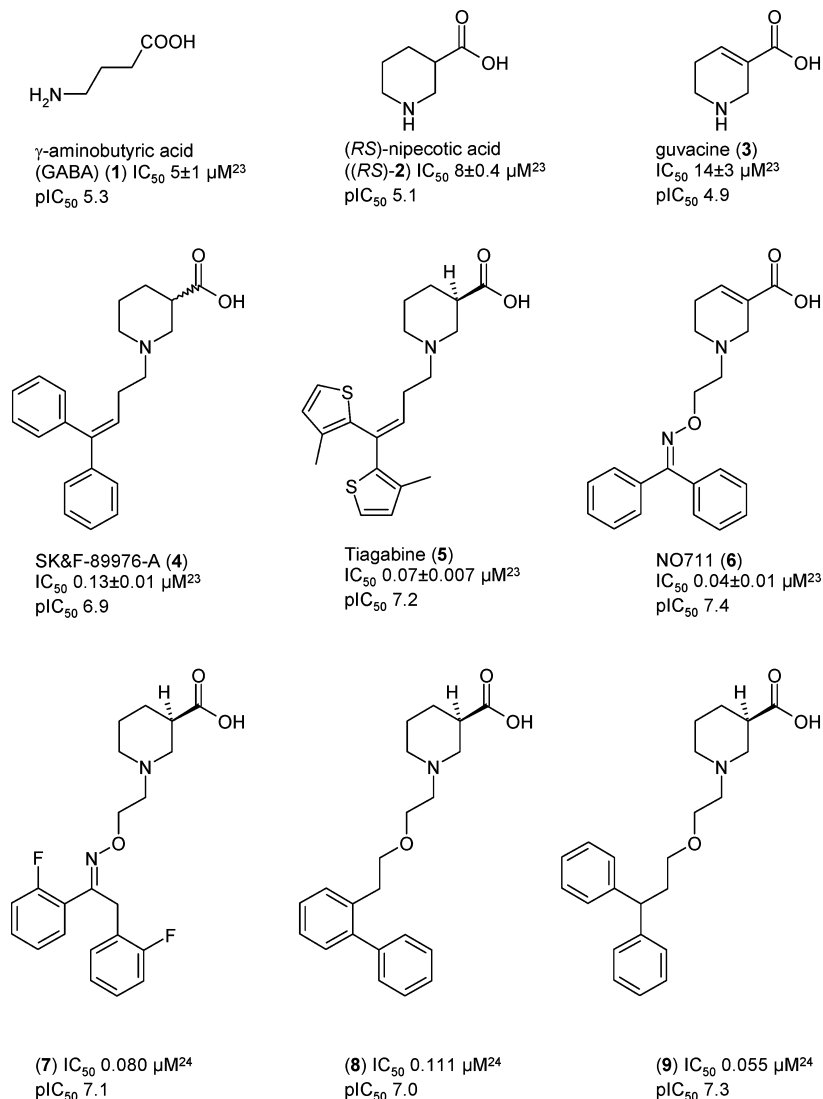
When GATs were defined as pharmacological CNS targets,¹⁷ a first generation of inhibitors was disclosed including cyclic analogues of GABA (**1**). These small cyclic amino acids like nipecotic acid (**2**) and guvacine (**3**) (Chart 1) were in the 1970s found to be potent in vitro inhibitors.^{18,19} Nevertheless, their potency was not confirmed in vivo because of their hydrophilic character preventing them from passing the blood–brain barrier in sufficient amount.²⁰ Consequently, a second generation of GAT inhibitors was born by substitution of the small amino acids with characteristic lipophilic side chains at the amino function that enabled them to cross the blood–brain barrier.²¹ Examples of the affinity enhancing side chains are represented in SK&F-89976-A (**4**), tiagabine (**5**), and NO711 (**6**) that proved to have high affinity at and subtype selectivity for mGAT1 compared to the nonsubstituted amino acids (Chart 1).²² In addition, **5** has successfully undergone clinical trials and is now in use as add-on medication for the treatment of epilepsy.²³

On the basis of this success, further selective and potent inhibitors were developed in the style of these potent GAT1 inhibitors representing the third generation of mGAT1 inhibitory drugs. These were characterized by new side chains

Received: December 7, 2012

Published: January 21, 2013

Chart 1. Structures of GABA and GAT1 Inhibitors



including the lipophilic aromatic domain attached to the amino group of the amino acid moiety (Chart 1). To this group belong a number of nipecotic acid based compounds in which the amino group of the hydrophilic amino acid moiety was connected via spacers differing in length and functionalities, like oxime and ether groups, to lipophilic aromatic residues. A selection of these third generation inhibitors, which had been developed by Andersen et al. in 1999 and 2001,²⁴ is displayed in Chart 1 (compounds 7–9).

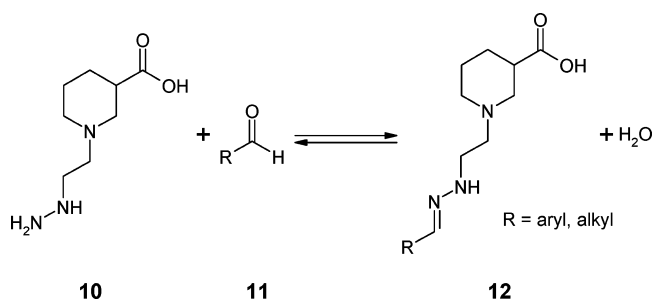
For GAT1, a screening method was developed several years ago that tested single drug candidates via a competitive MS binding assay, employing **6** as native MS marker.²⁵ This assay allowed the indirect determination of binding affinities toward GAT1 in analogy to radioligand binding studies, circumventing the necessity to apply radioactively labeled compounds.

Recently, we described a new method that applies MS binding assays,^{26,27} which so far had been used for the characterization of the binding affinities of single test compounds toward a target only, to the screening of compound libraries generated by efficient and the most fundamental reactions known from dynamic combinatorial chemistry (DCC).²⁸ Both library generation and screening were performed in the presence of the protein target to improve

assay performance. To facilitate hit detection, libraries were rendered pseudostatic. This was achieved by reacting sets of compounds with varying structure with a large excess of a single compound of complementary reactivity, thus generated one-dimensional libraries being almost constant in composition but still dynamic in nature. After library generation was performed, addition of a native MS marker to the same sample directly enabled detection of active libraries by MS binding assays. The feasibility of this concept was demonstrated for mGAT1, a well established target for which, as mentioned above, a MS binding assay utilizing **6** as native marker was already known.²⁵ Screening of libraries, each of which consisted of four hydrazone compounds **12** (Scheme 1) and had been generated by reacting nipecotic acid derived hydrazine **10** with four different aldehydes **11**, revealed new GAT1 inhibitors resembling structures **8** and **9** (Chart 1).

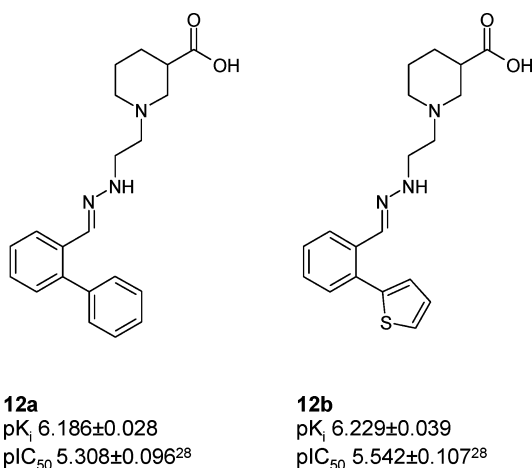
In this study, a specific limit of maximum remaining marker binding caused by $10 \mu M$ hydrazones was chosen to define a library as active. As such, a 20% level ($IC_{20} = 4 IC_{50}$) was selected that attributed a minimum potency (IC_{50}) of $2.5 \mu M$ to a single hydrazone based on the assumption that all other library members were inactive. In deconvolution experiments testing the single aldehydes in combination with hydrazine **10**,

Scheme 1. Condensation of Hydrazine Derived Nipecotic Acid Building Block **10** with Diverse Aldehydes **11**



out of each of the two libraries fulfilling this condition, a single hydrazone was identified to mostly represent the activity of the individual library. Thus, comparable to structure **8** (Chart 1) (*E*)-1-(2-{2-[1-(2',4'-dichlorobiphenyl-2-yl)methylidene]hydrazinyl}ethyl)piperidine-3-carboxylic acid (**12a**) (Chart 2)

Chart 2. Hydrazone Based GAT1 Inhibitors



resulting from the reaction of hydrazine **10** with biphenyl-2-carbaldehyde was found to reduce remaining marker binding in the deconvolution experiment to a value below the lower limit of quantification of the MS marker **6** (<5%), indicating an IC_{50} equal to or below 0.53 μM ($IC_{05} = 19 IC_{50}$). Resynthesis of **12a** and characterization in a full range competitive MS binding experiment finally revealed a pK_i of 6.186 ± 0.028 for this compound. The second hit, hydrazone **12b**, was derived from 2-thiophen-2-ylbenzaldehyde and gave rise to a remaining marker binding of $8.2 \pm 0.4\%$ in the deconvolution experiment and to a pK_i of 6.229 ± 0.039 in a full range competitive MS binding assay for the resynthesized compound.²⁸ That these mGAT1 binders are also functionally active was confirmed in [³H]GABA uptake assays with mGAT1 expressing HEK293 cells, the pIC_{50} values amounting to 5.308 ± 0.096 (**12a**) and 5.542 ± 0.107 (**12b**), respectively (Chart 2).

As we identified these two hits, **12a** and **12b**, with submicromolar potencies in the first library screening assays, the aim of the present study was to develop exemplarily for one of the two hits, compound **12a**, a focused library by introducing various substituents in the biaryl moiety to further optimize the affinity toward mGAT1 (Figure 1).

Biaryl focused pseudostatic hydrazone libraries (**12c–al**, Scheme 1) each derived from libraries of four biarylaldehydes (**11c–al**, Scheme 1) were therefore intended to be generated and subsequently screened by the MS binding assay, again employing **6** as native MS marker. As we aimed at improved affinities of desired hits compared to the hits searched in the first screening, the limit to define a library as active was further tightened by lowering it from 20% used in the original study²⁸ to 10%. In theory, this equals an IC_{50} of $\sim 1 \mu\text{M}$ to the compound, effecting reduction of marker binding to this limit when employed at 10 μM ($IC_{10} = 9 IC_{50}$). Hits contained in active libraries (<10% marker binding) were to be identified by applying the original deconvolution procedure and to be further evaluated after resynthesis.²⁸ As hydrazones are prone to hydrolysis,^{29,28} liver-toxic,^{30–32} and unstable against air,^{33–35} they are not suitable as lead structures for drug discovery. But the results obtained from the screening of hydrazone libraries

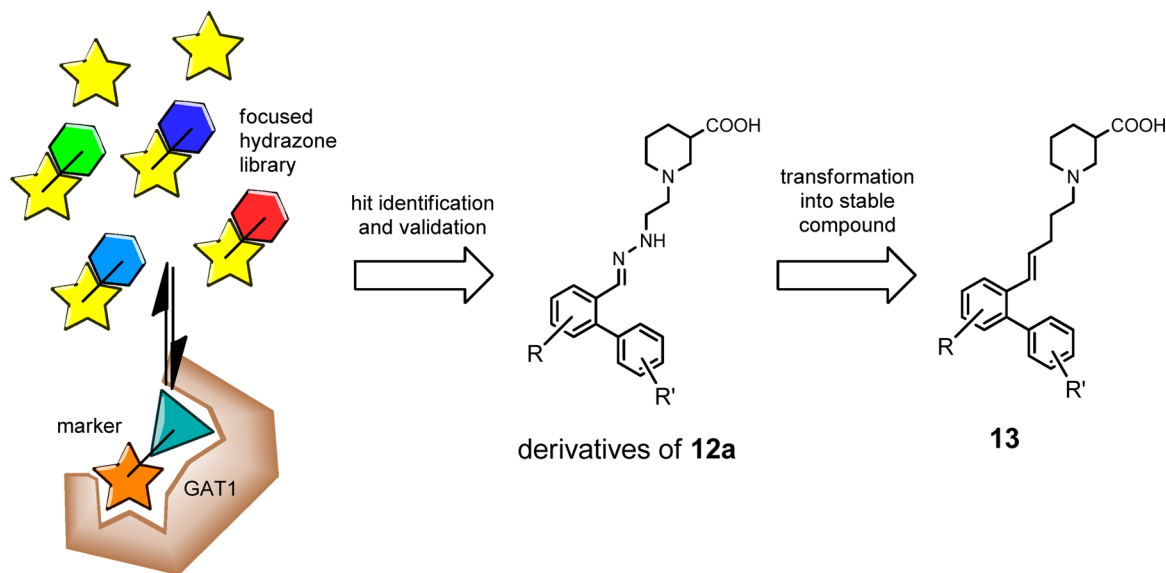
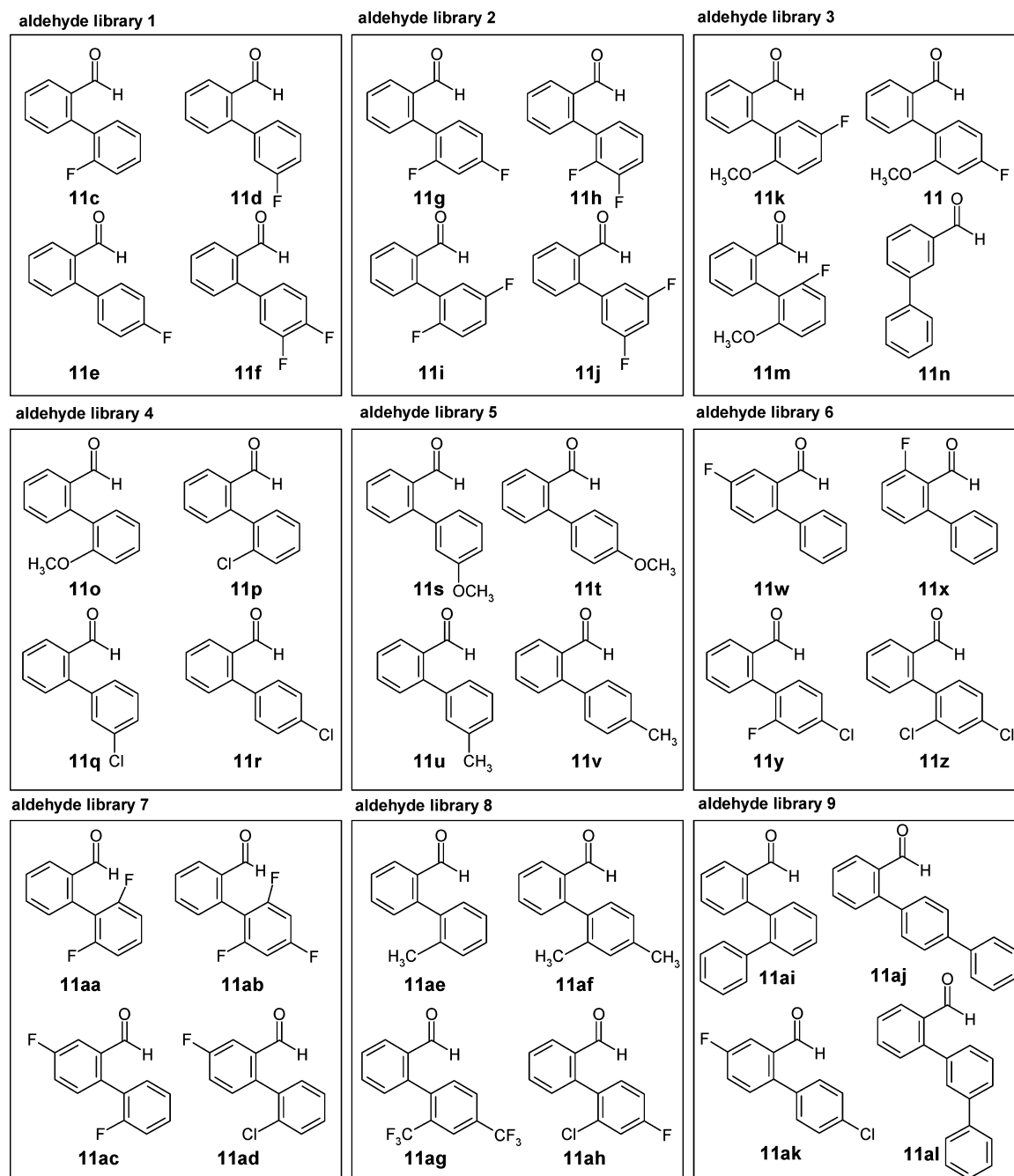


Figure 1. Focused hydrazone library generation and screening toward GAT1. After hit identification and validation of potent derivatives of hydrazone **12a**, corresponding carba analogues **13** were synthesized and evaluated.

Chart 3. Libraries Consisting of Biphenylcarbaldehydes 11c–al



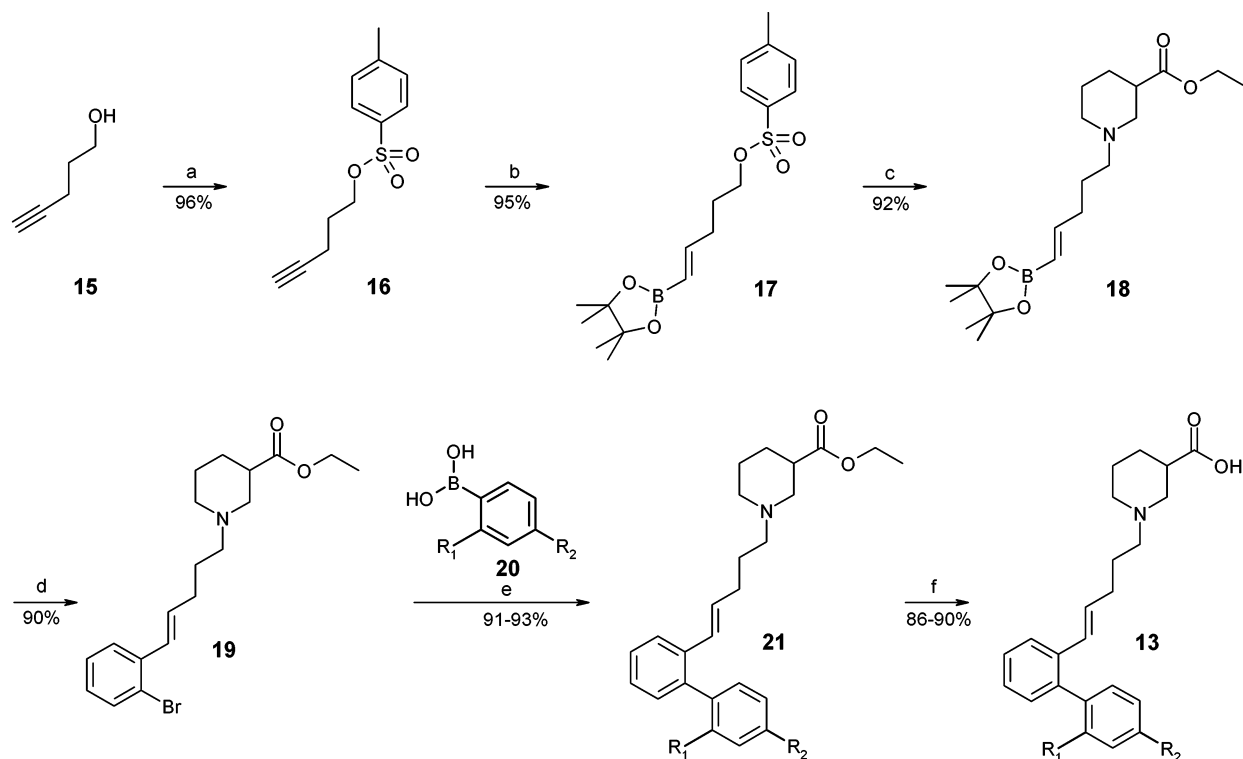
may nevertheless be of high value for drug discovery and support the development of stable analogues, which to demonstrate was a further aim of this study. Carba derivatives in which the hydrazone linker had been replaced by an all carbon chain with a double bond ($\text{CH}=\text{N}-\text{NH}-\text{CH}_2-\text{CH}_2 \rightarrow \text{CH}=\text{CH}-\text{CH}_2-\text{CH}_2-\text{CH}_2$) were considered a good choice as stable substitutes of the hydrazone inhibitors. Thus, the synthesis and biological evaluation of carba analogues of a series of representative hydrazone inhibitors were also included in this study.

■ CHEMISTRY

Synthesis of Biarylcarbaldehydes. In general, biphenylcarbaldehydes 11c–11al (Chart 3) required for library

generation were synthesized via the Suzuki–Miyaura³⁶ reaction except for 4'-fluorobiphenyl-2-carbaldehyde (11e) and biphenyl-3-carbaldehyde (11n) that were purchased from Alfa Aesar and Sigma-Aldrich, respectively.

Thus, 2'-fluorobiphenyl-2-carbaldehyde (11c)^{37,38} was obtained from 2-bromobenzaldehyde and 2-fluorophenylboronic acid, applying a literature method³⁹ that had been successfully employed in the synthesis of diversely substituted biphenyl-2-carbaldehydes (reaction conditions: 2-bromobenzaldehyde/substituted phenylboronic acid = 1:1, 5 mol % $\text{Pd}(\text{OAc})_2$, $\text{DMF}/\text{H}_2\text{O} = 2:1$, 25 °C). For the preparation of the biphenyl-2-carbaldehydes 11d, 11f, 11h, 11i, 11j, 11k, 11m, 11o, 11p, 11q, 11r, 11t, 11u, 11v, 11w, 11x, 11ac, 11ad, and 11ae this procedure had to be modified by adding common phosphine ligands (triphenylphosphine, dibenzylideneacetone, tri-*o*-tolyl-

Scheme 2. Synthesis of Nipecotic Acid Derived Carba Analogues 13^a

compd.	substitution	
	R ₁	R ₂
13, 20, 21		
c	F	H
g	F	F
p	Cl	H
ah	Cl	F
z	Cl	Cl

^aReagents and conditions: (a) TsCl, Et₃N, CH₂Cl₂, 0 °C to rt, 20 h; (b) pinacolborane, chloridobis(cyclopentadienyl)hydrido-zirconium no solvent, rt, 48 h; (c) ethyl nipecotate, no solvent, rt, 16 h; (d) Pd(dppf)Cl₂·CH₂Cl₂, 1-bromo-2-iodobenzene, K₂CO₃, 1,4-dioxane/H₂O 2:1, 72 h, rt; (e) Pd(dppf)Cl₂·CH₂Cl₂, RPhBO₂H, K₂CO₃, 1,4-dioxane/H₂O 2:1, 3 h, 60 °C; (f) NaOH, EtOH, 4 h, rt.

phosphine, or tri-*tert*-butylphosphine) and increasing the temperature from room temperature to 80 °C to improve the reaction rates and the yields (see Supporting Information).

The latter protocol could not be successfully applied to the synthesis of **11y** starting from 2-bromobenzaldehyde and 2-fluoro-4-chlorophenylboronic. But coupling of 2-bromobenzaldehyde and 2-fluoro-4-chlorophenylboronic acid to yield **11y** could be realized following a related literature method that had originally been used for coupling of pentafluorophenylboronic acid with halogenated benzene derivatives by means of CsF, Ag₂O, Pd(dba)₃·CHCl₃, and tri-*o*-tolylphosphine in pure DMF at 100 °C⁴⁰ (see Supporting Information).

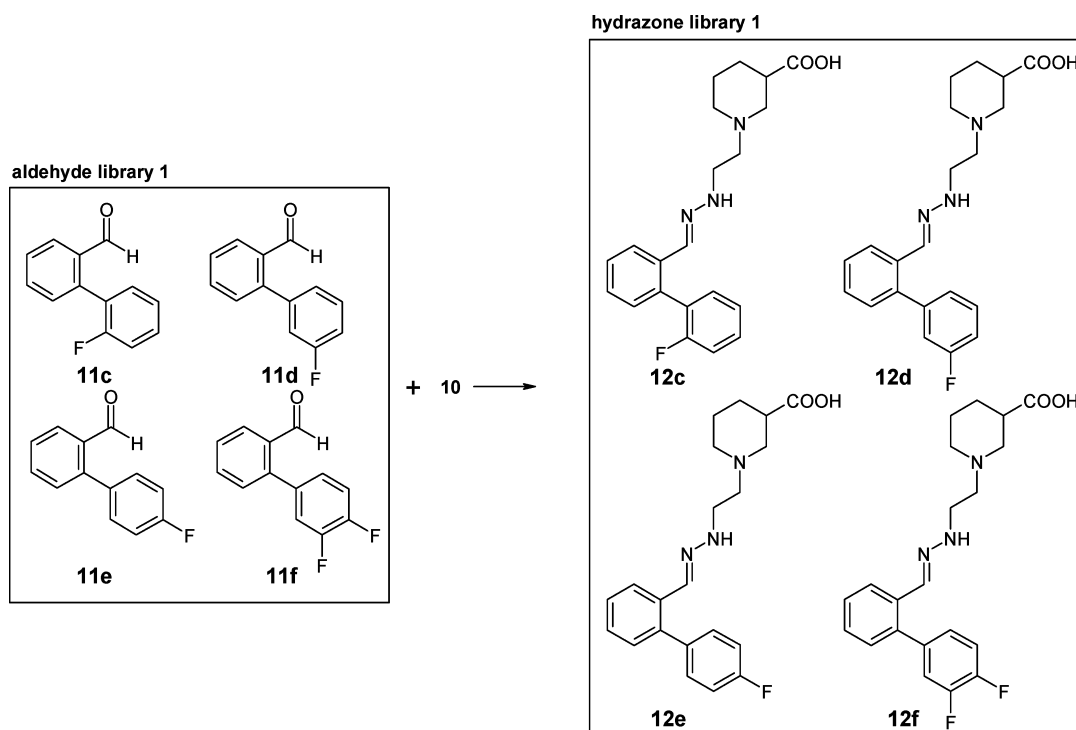
In the case of other sterically demanding phenylboronic acid derivatives carrying electron withdrawing residues (2,4-difluorophenylboronic acid, 2,4-dichlorophenylboronic acid, 2,6-difluorophenylboronic acid, 2,4,6-trifluorophenylboronic acid, 2-chloro-4-fluorophenylboronic acid), the coupling with 2-bromobenzaldehyde gave poor yields or no coupling products at all under the applied conditions for the preparation of, for example, **11d**. However, an alternative approach starting from 2-formylphenylboronic acid, instead of 2-bromobenzaldehyde,

and an appropriate halogenated benzene derivative instead of the corresponding phenylboronic acid gave access to the desired aldehydes. Thus, **11g**, **11z**, **11aa**, **11ab**, and **11ah** were obtained by reacting 2-formylphenylboronic acid with the appropriately halogen substituted benzene derivatives following a literature method that originally had been used for coupling of 1-bromo-2,3,4,5,6-pentafluorobenzene with 2-formylphenylboronic acid.⁴¹

The same reaction conditions that had been used for the coupling reactions of 2-formylphenylboronic acid with various aryl halides were finally also tested for the preparation of aldehydes **11s**, **11ab**, **11af**, **11ag**, **11ai**, **11aj**, **11ak**, and **11al** by coupling 2-bromobenzaldehyde again with the respective phenylboronic acid derivatives, leading to the desired compounds in yields of up to 90% (toluene/ethanol/2 M Na₂CO₃(aq) = 1:1:1, tetrakis(triphenylphosphine)-palladium(0)) (see Supporting Information).

Synthesis of the Hydrazones. Synthesis of individual hydrazones required for full scale competition experiments was carried out by combining 1 equiv of aldehyde with 1 equiv of hydrazine **10** according to Scheme 1, again following the

Scheme 3. Example for the Conversion of an Aldehyde Library into a Hydrazone Library (Aldehyde Library 1 → Hydrazone Library 1)



original protocol for hydrazone synthesis described previously.²⁸

Synthesis of the Carba Analogues. For the synthesis of the carba analogues of the hydrazone derivatives the reaction sequence outlined in Scheme 2 has been developed. It features the vinylboronic acid derivative **18** as a key compound, which by two consecutive Suzuki–Miyaura reactions allows high flexibility with regard to construction and the substitution pattern of the biaryl moiety present in the target compounds **13**. For the synthesis of **18**, first pentynol **15** was transformed into the tosyl ester **16** by reaction with TsCl according to a literature method.⁴² The resulting alkyne **16** was subsequently reacted with pinacolborane in the presence of Cp_2ZrHCl in analogy to a literature procedure,⁴³ to give the boronic acid ester **17**, which upon treatment with ethyl nipecotate provided **18** in 92% yield. Compound **18** allowed stepwise establishment of the biaryl moiety present in the final compounds **13**. Thus, a first Suzuki–Miyaura cross-coupling reaction between **18** and 1-bromo-2-iodobenzene yielded the monoaryl derivative **19**. Compound **19** was then subjected to a second Suzuki–Miyaura cross-coupling reaction with differently substituted phenylboronic acid derivatives [2-fluorophenylboronic acid (**20c**), 2,4-difluorophenylboronic acid (**20g**), 2-chlorophenylboronic acid (**20p**), 2-chloro-4-fluorophenylboronic acid (**20ah**), and 2,4-dichlorophenylboronic acid (**20z**)] to give the desired biaryl substituted nipecotic acid ester derivatives **21c**, **21g**, **21p**, **21ah**, and **21z** (yield 91–93%). These last compounds were finally converted to the free nipecotic acid derivatives **13c**, **13g**, **13p**, **13ah**, and **13z** by basic hydrolysis of the ethyl ester function (yield 86–90%).

RESULTS AND DISCUSSION

General Aspects of Library Generation and Screening.

Libraries were generated and screened as described earlier.²⁸

Therefore, the respective experimental conditions are given here only in short form. To generate the hydrazone libraries, aldehyde libraries of four aldehydes each at 10 μM were reacted with a 2.5-fold excess of hydrazine **10** (100 μM initial concentration) at 37 °C for 4 h, in which the time span had turned out to be sufficient for complete conversion in the former²⁸ and in the present study. In addition, library generation was again performed in the presence of the target mGAT1 to improve assay performance. The activity of the libraries was finally analyzed by means of competitive MS binding experiments. To this end, following incubation of libraries with MS marker **6** (for 40 min), the amount of specifically protein-bound MS marker **6** was quantified by LC–ESI-MS/MS (after isolation of protein–ligand complexes and liberation of the bound ligands from the target), low amounts of remaining marker binding representing high library activity and vice versa. As for the original procedure, in addition to each screening experiment, control experiments employing aldehyde libraries (**11**) and hydrazine **10**⁴⁴ alone were performed to ensure that the building blocks in the concentrations used do not affect marker binding to a remarkable extent.

Screening and Deconvolution of Focused Biphenyl-2-carbaldehyde Derived Hydrazone Libraries. In our former study²⁸ that applied pseudostatic hydrazone libraries on mGAT1, **12a**, the hydrazone derived from biphenyl-2-carbaldehyde (**11a**), had been uncovered to display sub-micromolar affinity to mGAT1 ($\text{pK}_i = 6.186 \pm 0.028$).²⁸ To further optimize the affinity of **12a** for mGAT1 in the present study, 36 aldehydes mainly delineated from biphenyl-2-carbaldehyde (**11a**) by additional small substituents in the phenyl rings (biphenylcarbaldehydes **11c–11al**) were selected for hydrazone generation and screening. These were grouped into nine libraries of four aldehydes (Chart 3), converted into hydrazone libraries (Scheme 3), and analyzed by competitive

MS binding assays as described above. Clearly, a higher number of aldehydes than four could be employed in library formation under otherwise identical conditions. But this would require reduction of the concentration of the individual aldehydes to further warrant the excess of hydrazine **10** over the aldehydes employed and thus the pseudostatic character of the libraries. However, with lowering hydrazone concentrations, the conditions for a library to be classified as active will also become more stringent (IC_{50} corresponds to the initial aldehyde concentration).

Table 1 summarizes the screening values of the aldehyde and hydrazone libraries 1–9. All hydrazone libraries were found to

Table 1. Library Screening Values of Aldehyde Libraries and Hydrazone Libraries

entry	library	library screening ^a (%)	
		aldehyde library	hydrazone library
1	library 1	82 ± 2	<5
2	library 2	81 ± 2	<5
3	library 3	88 ± 2	<5
4	library 4	79 ± 3	<5
5	library 5	91 ± 11	6 ± 1
6	library 6	85 ± 4	<5
7	library 7	35 ± 1	<5
8	library 8	81 ± 1	<5
9	library 9	81 ± 1	<5

^aPercentage of remaining specific binding of NO711 (**6**) in the presence of pure aldehyde libraries and corresponding hydrazone libraries after an incubation time of 4 h for library generation and 40 min for marker binding to mGAT1, $n = 4$, $\pm SD$, $<5\% = <50$ pM derived from the LLOQ of NO711 (50 pM, as 1–2 nM of 20 nM applied NO711 is maximally bound to the membrane preparation). Control experiment for 100 μM hydrazine **10** was obtained comparable to published results. See ref 28.

be highly active, reducing the remaining MS marker binding not only below 10%, the limit set for libraries to be considered as active, but even below the lower limit of quantitation (LLOQ) for the MS marker **6** of 5% (Table 1). Also library 5, which was the only exception, displayed a very low remaining marker binding of 6 ± 1%.

Showing very high activity in the screening step reducing MS marker binding below 10%, all libraries were also included in subsequent deconvolution experiments to identify the most active compounds. These experiments were performed analogous to the library screening except that single aldehydes were employed instead of the libraries.

In the deconvolution study of the hydrazone libraries, 21 of the 36 hydrazones were found to strongly influence MS marker binding, reducing it to 10% and below (Figure 2). Taking into account that a reduction of MS marker binding to 10% corresponds to an IC_{50} of ~ 1 μM ($IC_{10} = 9IC_{50}$), we considered it worthwhile to resynthesize most of the hydrazone derivatives that had reached this limit in the screening and to establish their pK_i values in MS competition experiments comprising complete competition curves. The data of these studies that had also been established to provide an improved insight on the influence of the substituent effects on the potency of the compounds are given in the section “Biphenyl-2-carbaldehyde Derived Hydrazone Hits”.

Interestingly, one of the pure aldehyde libraries (tested in the absence of hydrazine **10**) had also given rise to a significant

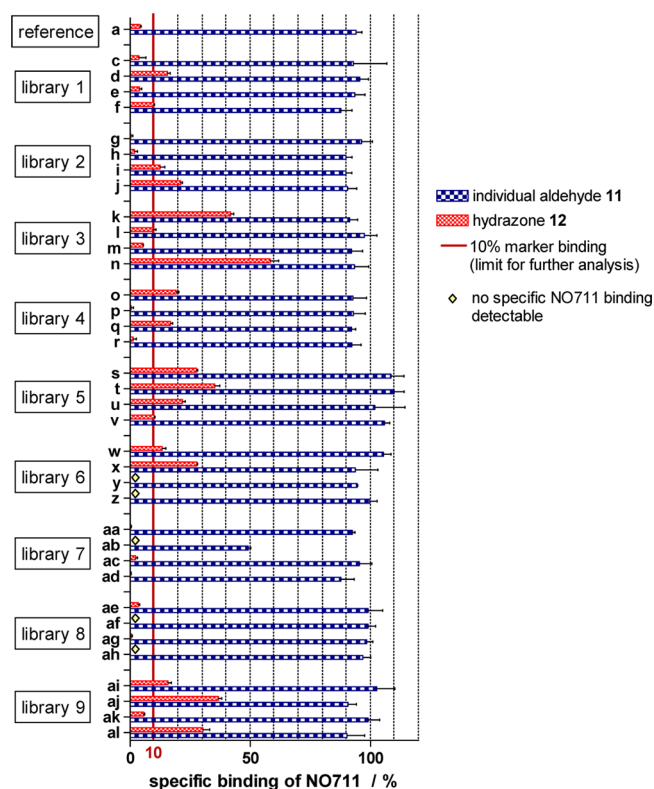


Figure 2. Deconvolution results of libraries 1–9. The limit for further analysis of a library was defined as 10% remaining marker binding.

reduction of MS marker binding. For aldehyde library 7 for which the screening value had amounted to 35 ± 1% (Table 1, entry 7), a deconvolution experiment (in the absence of hydrazine **10**) revealed aldehyde **11ab** to be by far the most potent binder of this group, reducing MS marker binding to 49 ± 1% (Figure 2). Accordingly, as a rough estimate, an IC_{50} of ~ 10 μM can be attributed to this aldehyde.²⁸

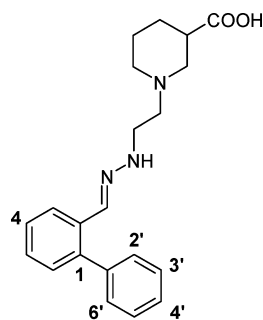
Biphenyl-2-carbaldehyde Derived Hydrazone Hits

Table 2 summarizes the pK_i values that had been found in full scale competitive MS binding assays for the separately resynthesized biphenyl-2-carbaldehyde derived hydrazones that had turned out as the most active ligands at mGAT1 in the deconvolution experiments (reduction of MS marker binding to $\leq 10\%$). Hydrazones **12d**, **12i**, **12j**, **12k**, **12n**, **12o**, **12q**, **12s**, **12t**, **12u**, **12w**, **12x**, **12ai**, **12aj**, and **12al** did not reach this limit and were excluded from further analysis.

The compounds that achieved the desired value below 10% are sorted according to the substituents of the biaryl moiety starting with hydrazones exhibiting only F-substituents (Table 2, entries 2–9), F- and CH_3O -substituents (Table 2, entries 10 and 11), followed by those with either CH_3 - (Table 2, entries 12–14), CF_3 - (Table 2, entry 15), Cl- (Table 2, entries 16–18), or F- and Cl-substituents (Table 2, entries 19–22).

An F-substituent in the 2'-position increased the affinity by almost 1 order of magnitude, resulting in a pK_i of 6.914 ± 0.061 for **12c** (Table 2, entry 2) compared to the parent compound **12a** (6.186 ± 0.028 , Chart 2, Table 2, entry 1), while a 4'-F-substituent (structure **12e**) caused a smaller increase, the affinity of **12e** amounting to a pK_i of 6.546 ± 0.067 (Table 2, entry 3). With F-substituents present in both the 2'- and 4'-position, a gain in binding energy (compared to **12a**) was observed that was roughly the sum of the increase of binding energies effected by the two F-substituents in **12c** and **12e**,

Table 2. Binding affinities (pK_i) of Resynthesized Biphenyl Derived Hydrazones Determined from Competitive MS Binding Assays and Inhibitory Potencies (pIC_{50}) at mGAT1 from [3H]GABA Uptake Experiments



12a

entry	compd	compd ^a (substitution pattern of the biphenyl moiety of 12a)					biological testing	
		4	2'	3'	4'	6'	binding affinity pK_i ($n = 3 \pm SEM$) ^b	inhibitory potency pIC_{50} ^c ($n = 3 \pm SEM$) ^b
1	12a	H	H	H	H	H	6.186 ± 0.028	5.308 ± 0.096
2	12c	H	F	H	H	H	6.914 ± 0.061	6.277 ± 0.061
3	12e	H	H	H	F	H	6.546 ± 0.067	5.746 ± 0.078
4	12g	H	F	H	F	H	7.449 ± 0.023	6.891 ± 0.078
5	12h	H	F	F	H	H	6.690 ± 0.036	5.824 ± 0.033
6	12f	H	H	F	F	H	6.204 ± 0.054	5.479 ± 0.095
7	12aa	H	F	H	H	F	6.883 ± 0.035	6.001 ± 0.014
8	12ab	H	F	H	F	F	7.514 ± 0.030	6.594 ± 0.046
9	12ac	F	F	H	H	H	6.578 ± 0.057	5.763 ± 0.037
10	12m	H	F	H	H	OCH ₃	6.354 ± 0.062	5.648 ± 0.103
11	12l	H	OCH ₃	H	F	H	6.119 ± 0.037	5.134 ± 0.094
12	12ae	H	CH ₃	H	H	H	6.666 ± 0.044	5.806 ± 0.064
13	12v	H	H	H	CH ₃	H	6.325 ± 0.065	5.468 ± 0.118
14	12af	H	CH ₃	H	CH ₃	H	7.135 ± 0.095	6.078 ± 0.020
15	12ag	H	CF ₃	H	CF ₃	H	6.769 ± 0.081	5.549 ± 0.047
16	12p	H	Cl	H	H	H	7.184 ± 0.063	6.320 ± 0.070
17	12r	H	H	H	Cl	H	6.762 ± 0.001	6.012 ± 0.121
18	12z	H	Cl	H	Cl	H	8.094 ± 0.098	7.213 ± 0.085
19	12ad	F	Cl	H	H	H	6.981 ± 0.060	5.909 ± 0.081
20	12ak	F	H	H	Cl	H	6.630 ± 0.040	5.708 ± 0.078
21	12y	H	F	H	Cl	H	7.607 ± 0.043	6.899 ± 0.147
22	12ah	H	Cl	H	F	H	7.835 ± 0.081	6.535 ± 0.082

^aIndividually resynthesized from appropriate biphenyl-2-carbaldehydes and evaluated hydrazones. ^bData points for specific binding of NO711 (mean ± SD from triplicate values) in the presence of different concentrations of test compounds (M) resulted in binding curves for K_i determination by nonlinear regression. $pK_i \pm SEM$ obtained from three independent experiments. ^c pIC_{50} values from [3H]GABA uptake assays performed with mGAT1 expressing HEK293 cells. Value ± SEM obtained from three independent experiments.

hydrazone **12g** displaying a pK_i of 7.449 ± 0.023 (Table 2, entry 4). Comparing this effect with the difluoro substitution in **12h** ($2',3'-F_2$, Table 2, entry 5), **12f** ($3',4'-F_2$, Table 2, entry 6), and **12aa** ($2',6'-F_2$, Table 2, entry 7), the pK_i values of the compounds amounting to 6.690 ± 0.036 , 6.204 ± 0.054 , and 6.883 ± 0.035 , respectively, clearly reveals that the $2',4'-F_2$ substitution in **12g** represents the most favorable substitution pattern for the difluoro substituted compounds. In contrast to F-substituents in $2'$ - and $4'$ -position, a $3'$ -F-substituent decreases affinity compared to the parent compound **12a**, with hydrazone **12d** reducing MS marker binding in the deconvolution experiments far less ($16 \pm 1\%$, **12d**, Figure 2) than the reference compound **12a** ($<5\%$). In line with that, upon transition from the $2'$ -F-substituted **12c** ($pK_i = 6.914 \pm 0.061$, Table 2, entry 2) to the $2',3'-F_2$ hydrazone **12h**, a decrease in affinity occurs ($pK_i = 6.690 \pm 0.036$, Table 2, entry 5). But the positive effect of the $2'$ -F-substituent clearly

outweighs the negative effect of the $3'$ -F-substituent as the affinity of **12h** is still far higher than that of the parent compound **12a** (Table 2, entry 1). In addition, **12aa** ($2',6'-F_2$, Table 2, entry 7) revealed that a second F-substituent in $6'$ -position is tolerated but does not improve the affinity toward mGAT1, expressed by a pK_i of 6.883 ± 0.035 very close to the pK_i of **12c** ($2'-F_2$ $pK_i = 6.914 \pm 0.061$, Table 2, entry 2). Accordingly, the $2',4',6'$ -trifluoro substituted derivative **12ab** ($2',4',6'-F_3$, Table 2, entry 8), displayed a similar affinity, the pK_i being 7.514 ± 0.030 , close to that of **12g** ($2',4'-F_2$, $pK_i = 7.449 \pm 0.023$, Table 2, entry 4), again indicating that a $6'$ -F-substituent does not significantly change affinity. Obviously a $4'$ -F-substituent in the first ring does not lead to a beneficial effect, the affinity of the $4,2'$ -difluoro substituted hydrazone **12ac** (Table 2, entry 9) with a pK_i of 6.578 ± 0.057 being lower than that of the $2'$ -monofluoro substituted hydrazone **12c** ($2'-F$, 6.914 ± 0.061 , Table 2, entry 2). Like the 4-fluoro substituent

in **12ac**, the 4-fluoro substituent in hydrazone **12w** also has a negative effect on the binding affinity, which in the latter case was even more pronounced reducing remaining MS marker binding to only $13 \pm 2\%$ in the deconvolution experiments, thus not reaching the limit of 10%, which is the condition hydrazones had to fulfill to be evaluated with regard to their pK_i values.

A methoxy function in 6'-position of the 2'-fluoro substituted system (2'-F,6'-OCH₃, **12m**, Table 2, entry 10) had an adverse effect on the affinity, as well, the pK_i value of **12m** ($pK_i = 6.354 \pm 0.062$) ranging distinctly below that of the 2'-fluoro monosubstituted compound **12c** ($pK_i = 6.914 \pm 0.061$, Table 2, entry 2) and close to that of the parent compound **12a** ($pK_i = 6.186 \pm 0.028$, Table 2, entry 1). This was not unexpected as the 2'-OCH₃ substituted hydrazone **12o** had reduced MS marker binding in the deconvolution experiments no lower than $19 \pm 1\%$. Anyway, the gain in binding affinity effected by the 2'-fluoro substituent in **12c** (2'-F) was nearly completely abolished by the additional 6'-OCH₃ substituent (in **12m**). A similar effect was observed for **12l**. The additional 2'-OCH₃-residue, by which this compound differs from **12e**, exhibiting a 4'-F-substituent, causes a pK_i reduction from 6.546 ± 0.067 (of **12e**, Table 2, entry 3) to 6.119 ± 0.037 (**12l**, Table 2, entry 11), **12l** thus being just as potent as the parent compound **12a** ($pK_i = 6.186 \pm 0.028$, Table 2, entry 1).

Compared to a 2'-F substituent (**12c**, 2'-F, $pK_i = 6.914 \pm 0.061$, Table 2, entry 2), the binding enhancing effect of a 2'-CH₃ is less pronounced (**12ae**, $pK_i = 6.666 \pm 0.044$, Table 2, entry 12). The 4'-CH₃ substituted hydrazone **12v** (4'-CH₃) gave rise to a pK_i of 6.325 ± 0.065 (Table 2, entry 13), the 4'-CH₃ substituent thus having slightly improved the potency of the parent compound **12a** ($pK_i = 6.186 \pm 0.028$, Table 2, entry 1) though the deconvolution value (percentage of remaining MS marker binding) of **12v** amounting to $10 \pm 1\%$ had been higher than that of **12a** ($<5\%$), suggesting the opposite effect. This discrepancy is possibly attributed to the uncertainties of the experimental data that are commonly relatively large for biological systems. The positive effects of the 2'-methyl (as in **12ae**, 2'-CH₃) and the 4'-methyl group (as in **12v**, 4'-CH₃) were combined in the 2',4'-disubstituted hydrazone **12af** (2',4'-CH₃, Table 2, entry 14), reaching an affinity of $pK_i = 7.135 \pm 0.095$. Among the 2',4'-disubstituted derivatives, **12ag** (2',4'-(CF₃)₂) exhibiting two CF₃ groups was also found to be more potent than the parent compound **12a** ($pK_i = 6.186 \pm 0.028$, Table 2, entry 1) displaying a pK_i of 6.769 ± 0.081 (Table 2, entry 15) but less than the 2',4'-dimethyl and 2',4'-difluoro substituted hydrazones **12af** and **12g** (**12af**, 2',4'-(CH₃)₂, $pK_i = 7.135 \pm 0.095$, Table 2, entry 14; **12g**, 2',4'-F₂, $pK_i = 7.449 \pm 0.023$, Table 2, entry 4).

The largest increase in affinity by a single substituent was observed for a 2'-Cl residue, the respective compound **12p** (2'-Cl, Table 2, entry 16) achieving a pK_i of 7.184 ± 0.063 close to that of the 2',4'-difluoro substituted derivative (**12g**, $pK_i = 7.449 \pm 0.023$, Table 2, entry 4). An additional 4-F-substituent in the first ring again gave rise to a reduced affinity (**12ad**, 4-F,2'-Cl $pK_i = 6.981 \pm 0.060$, Table 2, entry 19), in line with the results described above. The affinity of the 4'-Cl biphenylhydrazone **12r** (4'-Cl) with a pK_i of 6.762 ± 0.001 (Table 2, entry 17) was also higher than that of the 4'-F substituted analogue **12e** ($pK_i = 6.546 \pm 0.067$, Table 2, entry 3). An additional 4-F substituent again led to a decrease in affinity, the pK_i of **12ak** (4-F,4'-Cl, $pK_i = 6.630 \pm 0.040$, Table 2, entry 20) being lower than that of **12r** with a single 4'-Cl substituent ($pK_i = 6.762 \pm$

0.001 , Table 2, entry 17). But this decrease was less pronounced than that for the transition from **12p** (2'-Cl, Table 2, entry 16) to **12ad** (4-F,2'-Cl, Table 2, entry 19).

Combining the 2'- and the 4'-Cl-substitution in one compound led to the most potent biphenylhydrazone of this study, compound **12z** (2',4'-Cl₂), with an affinity in the lower nanomolar range ($pK_i = 8.094 \pm 0.098$, Table 2, entry 18), as the pK_i of this hydrazone derivative surpassed that of the parent compound **12a** ($pK_i = 6.186 \pm 0.028$, Table 2, entry 1) by almost 2 log units.

Further high affinity ligands were obtained by mixed halogen substitution of the 2',4'-position of the biphenyl moiety in **12a**. Compound **12ah**, the 2'-Cl,4'-F substituted compound, turned out to be the second most potent biphenylhydrazone derivative of this series ($pK_i = 7.835 \pm 0.081$, Table 2, entry 22) followed by **12y** (2'-F,4'-Cl), exhibiting the reverse halogen substitution pattern, with a slightly diminished potency ($pK_i = 7.607 \pm 0.043$, Table 2, entry 21).

In conclusion of these results, substitution in 2',4'-position of the biphenyl moiety was most favorable to gain highly potent derivatives of the parent compound **12a**. Most of all, the presence of halogen substituents such as F and even more Cl in these positions augmented binding affinities remarkably. This is best underlined by the high affinity displayed by the 2',4'-Cl₂ biphenylhydrazone **12z** (2',4'-Cl₂, $pK_i = 8.094 \pm 0.098$, Table 2, entry 18). Besides, as demonstrated by these results, the screening data are in general in good accord with the results of the MS binding assays and can thus already be considered a good estimate for the potency of the studied compounds.

In addition to their binding affinities (pK_i values) all compounds were also characterized with respect to their inhibitory potencies (IC₅₀) in functional [³H]GABA uptake assays performed with mGAT1 expressing HEK293 cells. As already stated in previous papers,²⁸ the pIC₅₀ values of the uptake assay are generally lower than the pK_i values describing the binding affinity. This may be ascribed to the different assay conditions used for the [³H]GABA uptake and for the MS binding assays. Most importantly MS binding assays are performed in a buffer system containing 1 M NaCl whereas for [³H]GABA uptake assays a physiological buffer with 120 mM NaCl is used.⁴⁵ The high NaCl concentration in the MS binding assays is needed to improve ligand affinity of the MS marker **6**, which is otherwise, when NaCl is present in physiological concentration (like in the buffer for the [³H]GABA uptake assay), about 1 log unit lower^{25,49} under which conditions these assays were more difficult to perform (to avoid uncontrolled loss of specifically bound MS marker **6** during the separation of the protein–ligand complex from the rest of the incubation system).

As the high NaCl concentration (1 M) affects the affinity of every test compound in a manner similar to the affinity of the MS marker **6**, their pK_i values being a half to 1 log unit higher than those measured in the presence of physiological NaCl concentration, the differences observed between the pK_i values from MS binding assays (in the presence of 1 M NaCl) and the pIC₅₀ values from [³H]GABA uptake assays (in the presence of physiological NaCl concentration) can be largely ascribed to this phenomenon. Regardless of that, the rank order of potency that results from the pIC₅₀ values of the [³H]GABA uptake assays is in good accord with that resulting from the pK_i values of the MS binding assays. Thus, in line with that, hydrazone **12z**, which displays the highest binding affinity (pK_i) for mGAT1 of the compounds studied, turned out to also be the

Table 3. Comparison of hydrazones 12c, 12p, 12g, 12z, 12ah with Carba Analogues 13c, 13p, 13g, 13z, 13ah

12					
pK_i^a	6.914±0.061	7.184±0.063	7.449±0.023	7.834±0.081	8.094±0.098
pIC_{50}^b	6.277±0.061	6.320±0.070	6.861±0.078	6.535±0.082	7.231±0.085
13					
pK_i^a	6.189±0.020	6.079±0.037	6.228±0.014	6.505±0.039	6.930±0.021
pIC_{50}^b	5.477±0.095	5.448±0.105	5.547±0.032	5.399±0.052	6.114±0.107

^aData points for specific binding of NO711 (mean ± SD from triplicate values) in the presence of different concentrations of test compounds (M) resulted in binding curves for K_i determination by nonlinear regression. $pK_i \pm$ SEM obtained from three independent experiments. ^b pIC_{50} values from [³H]GABA uptake assays performed with mGAT1 expressing HEK293 cells. Value ± SEM obtained from three independent experiments.

most potent inhibitor in the [³H]GABA uptake assay of mGAT1 expressing HEK293 cells, its pIC_{50} amounting to 7.213 ± 0.085 (Table 2, entry 18).

Carba Analogues for Biphenyl Derived Hydrazones.

The final step of this study was aimed at the development of stable analogues of the hydrazone derivatives that can substitute the latter as lead structure for drug development, a purpose hydrazones are in general not suitable for because of their instability^{28,33–35} and various harmful effects.^{30–32}

A carba moiety in which the two nitrogen atoms of the hydrazone function (CH=N–NH) are replaced by carbon atoms transforming said function into an allyl group (CH=CH–CH₂) was considered to be a suitable substitute that at least with respect to the overall geometry should be able to mimic the original functional group. For this transformation a set of hydrazone derivatives was selected covering diverse activities ranging from medium to highly potent. Thus, for the hydrazones 12c, 12p, 12g, 12ah, and 12z the corresponding carba analogues 13c, 13p, 13g, 13ah, and 13z were synthesized (Table 3) and evaluated.

As shown in Table 3, the potencies of the hydrazone derivatives 12c, 12p, 12g, 12ah, and 12z ranging from pK_i of 6.914 ± 0.061 (12c) to 8.094 ± 0.098 (12z) were not fully reached by the carba analogues 13c, 13p, 13g, 13ah, and 13z, the pK_i values of the latter compounds being roughly 1 log unit lower than those of the corresponding hydrazone derivatives. But the rank order of potency remained mostly unchanged. Thus, also for the carba analogues, the 2',4'-dichloro substituted derivative 13z appeared to be the most potent compound in this series with a pK_i of 6.930 ± 0.021 followed by the 2'-chloro-4'-fluorocarba derivative 13ah (pK_i of 6.505 ± 0.039) and the 2',4'-difluorocarba derivative 13g (pK_i of 6.228 ± 0.014). The rank order of potency for the carba analogues was in line with the respective rank order of potency for the hydrazones. Only the 2'-fluoro (13c, pK_i = 6.189 ± 0.020) and the 2'-chloro substituted carba analogue (13p, pK_i = 6.079 ±

0.037) deviated from the rank order of potency observed for the hydrazone derivatives, this time the 2'-fluoro derivative 13c being more potent than the 2'-chloro derivative 13p. But similar to the hydrazone derivatives 12c and 12p, the differences in potencies were also very small for the carba analogues 13c and 13p, rendering this change in the rank order of potency less meaningful.

The carba analogues were finally also characterized with respect to their potencies in [³H]GABA uptake assays (Table 3). Again the pIC_{50} values for the [³H]GABA uptake assays were somewhat lower than the corresponding pK_i values resulting from the MS binding assays, the reasons for this phenomenon being most likely those given in the section "Biphenyl-2-carbaldehyde Derived Hydrazone Hits". The sequence of potencies (pIC_{50}) was roughly in line with that of the affinities (pK_i) found for these compounds, 13c, 13p, and 13g being nearly equally potent (13c, pIC_{50} = 5.477 ± 0.095; 13p, pIC_{50} = 5.448 ± 0.105, 13g, pIC_{50} = 5.547 ± 0.032), whereas 13z showed an increased potency (13z, pIC_{50} = 6.114 ± 0.107). Only 13ah (pIC_{50} = 5.399 ± 0.052) was slightly less potent than expected and equipotent to 13c, 13p, and 13g.

According to the results described above, structure–activity data obtained from screening of hydrazone libraries represent valuable information regarding drug target binding which can be used for the construction of stable analogues as lead structures but should also be useful in guiding the optimization of these compounds. The reduced potency of the carba analogues versus the parent screening hits is attributed to the lower polarity of the all-carbon spacer and possibly also to its inability to participate in hydrogen bonds in contrast to the hydrazone function.

CONCLUSION

Recently, competitive MS binding assays have been shown to be applicable as a readout for the screening of compound

libraries, generated by simple and most efficient reactions commonly used in dynamic combinatorial chemistry. A key feature of this method is to take special means to render the libraries pseudostatic in order to obtain well-defined library compositions with almost equal concentrations of test compounds. Furthermore, by generation of the libraries in the presence of the target under conditions appropriate for the MS binding assay, library generation and screening are performed in the same sample, thus enhancing the assay performance. When this concept was applied to mGAT1 as target employing pseudostatic hydrazone libraries, two hits, hydrazones **12a** and **12b**, were identified as moderate (submicromolar) binders of mGAT1. Both hits displayed a biaryl system representing the lipophilic part that was attached via a spacer to a more polar residue, in the present case a nipecotic acid moiety that is characteristic of most mGAT1 inhibitors. The aim of the current study was to further improve the affinities for mGAT1 by optimizing the biphenyl system of **12a**, one of the two hits that had been identified in the first screening round. Accordingly, focused hydrazone libraries comprising compounds with differently substituted biphenyl moieties were generated under pseudostatic conditions and screened by the aforementioned method developed for mGAT1 which is based on competitive MS binding experiments utilizing NO711 (**6**) as native MS marker. The screening of 9 biaryl focused pseudostatic hydrazone libraries comprising 36 hydrazones revealed 21 hydrazone hits with higher affinities than the original lead system **12a** ($pK_i = 6.186 \pm 0.028$). The most potent hit, **12z**, displaying a 2',4'-dichloro substituted biphenyl moiety, exhibited an affinity in the lower nanomolar range, the $pK_i = 8.094 \pm 0.098$ being almost 2 log units higher than of the original compound **12a**. Actually, 2',4'-disubstituted biphenyl units appeared to be most favorable for increased binding affinities toward mGAT1 with Cl and F substituents being most rewarding. A set of representative metastable hydrazone derivatives was chosen to explore the suitability of these compounds as models for the construction of stable analogues as lead structures for further drug development. Of five representative biphenylhydrazones the corresponding stable carba analogues were synthesized and tested in competitive MS binding experiments and [^3H]GABA uptake assays. Again, a 2',4'-dichloro substituted compound, i.e., **13z**, was found to be the most potent mGAT1 binder ($pK_i = 6.930 \pm 0.021$), though the pK_i value of **13z** was 1 log unit lower than that of the hydrazone derivative **12z**. This is possibly a result of the reduced polarity of the carba analogue compared to the corresponding hydrazone derivative. But pleasingly, the rank order of potency of the five carba analogues in the binding studies was the same as that of the corresponding hydrazone derivatives. Thus, this study clearly demonstrated that screening of focused hydrazone libraries under pseudostatic conditions is a powerful tool to detect hits and that these can be successfully used as a starting point for the development of almost equally potent lead structures.

EXPERIMENTAL SECTION

Chemistry. Solvents used were of analytical grade and freshly distilled before use except for DMSO. Ethyl nipecotate was purchased from Sigma-Aldrich and freshly distilled before use. Other purchased reagents and reactants were used without further purification. TLC was carried out on precoated silica gel F_{254} glass plates (Merck). Flash column chromatography (CC) was performed on Merck silica gel 60 (mesh 0.040–0.063 mm). Solvents used for elution are reported in

parentheses. ^1H NMR spectra were recorded on a JNM-RX (JEOL, 400 or 500 MHz) at room temperature unless otherwise described. DMSO- d_6 was applied for at least 5 min to ultrasonic degassing before use. ^1H chemical shifts were internally referenced to TMS or MeOH for samples solved in D_2O or CD_3OD . The spectra were processed with the NMR software MestReNova (version 5.1.1-3092, 2007, Mestrelab Research S. L., Santiago de Compostela, Spain). Broadened signals in ^1H NMR spectra were supplemented by the index "br" (s_{br} , d_{br} , t_{br}). IR spectroscopy was performed with an FTIR spectrometer 410 (Jasco). Samples were measured either as KBr pellets or as films on NaCl plates. A Hewlett-Packard 5989 A with 59.980 B particle beam LC-MS interface was used for mass spectrometry (ionization: chemical (CH_5^+) or electron impact (70 eV)). High resolution mass spectrometry was carried out with a LTQ-FT (ThermoFinnigan), FAB (Xenon, 6 kV, MBA, reference PEG), or a JMS GCmate II (Jeol). Purity testing was done by means of analytical HPLC on an Agilent 1100 instrument (G1329A ALS autosampler, G1316A column compartment, G1315B DAD detector, G1312A binary pump, G1322A degasser), equipped with a Lichrospher 100 RP-18 (5 μm) in a LiChroCART 125-4 column, with elution at 1 mL/min with phosphate buffer (5 mM $\text{NaH}_2\text{PO}_4 \cdot \text{H}_2\text{O}$, 5 mM $\text{Na}_2\text{HPO}_4 \cdot 2\text{H}_2\text{O}$, pH 7.0) to CH_3CN 40:60. Carba analogues **13c**, **13g**, **13p**, **13z**, **13ah** were $\geq 95\%$ pure. Because of the tendency of hydrazones to hydrolyze, necessitating specific means to render compound libraries pseudostatic, HPLC analysis did not appear to be reasonable. Because of autoxidation of hydrazones and hydrazines, starting material and products were stored under Ar.

General Procedure for the Preparation of Hydrazones (GP1).

According to the published procedure,²⁸ 1 equiv of the corresponding aldehyde in DMSO- d_6 ($c = 0.1$ M) was added to hydrazine **10**. For practical reasons NMR spectra were directly measured from this solution after at least five min. When all NMR measurements were finished, DMSO- d_6 was evaporated to give the desired hydrazone.⁴⁶ According to ^1H NMR spectra, hydrazones existed to $\geq 98\%$ as *E*-isomers.

General Procedure for the Suzuki Coupling of **19** and Phenylboronic Acid Derivatives (GP2).

Under nitrogen atmosphere Pd(dppf) $\text{Cl}_2 \cdot \text{CH}_2\text{Cl}_2$ (0.015 mmol, 5 mol %), the appropriate phenylboronic acid derivative (0.33 mmol), and compound **19** (114 mg, 0.300 mmol) were dissolved in 1,4-dioxane (0.6 mL), K_2CO_3 (124 mg, 0.90 mmol), and 0.3 mL of water. The resulting mixture was heated to 60 °C and stirred for 3 h. After addition of water (5 mL) the mixture was extracted three times with CH_2Cl_2 (5 mL). The combined organic layers were dried over Na_2SO_4 , and the solvent was evaporated in vacuo. The crude product was purified by flash column chromatography on silica gel (*n*-pentane/ CH_2Cl_2 /EtOAc = 8/1/1 + 2% Et_3N).

General Procedure for the Hydrolysis of N-Substituted Piperidine-3-carboxylic Acid Ethyl Ester Derivatives **21** (GP3).

The chosen piperidine-3-carboxylic acid ethyl ester derivative (0.2 mmol) was dissolved in EtOH (0.8 mL) followed by addition of NaOH (24.0 mg, 0.60 mmol, 0.050 mL, 12 M aqueous) (TLC monitoring). Upon completion of the reaction (approximately 4 h) water (5 mL) was added and the basic solution was washed with Et_2O (5 mL). Afterward the pH of the aqueous phase was adjusted to pH 6 with 1 M HCl and phosphate buffer solution (1 M, pH 7) and the product was extracted several times with CH_2Cl_2 . The combined organic layers were dried over Na_2SO_4 , and the solvent was removed in vacuo to give the appropriate product.

(E)-1-(2-{2-[1-(2'-Fluorobiphenyl-2-yl)methylidene]hydrazinyl}ethyl)piperidine-3-carboxylic Acid (12c**).** According to GP1 from hydrazine **10** (8.71 mg, 46.5 μmol) and **11c** (9.31 mg, 46.5 μmol), **12c** was obtained as colorless, amorphous solid (17.2 mg, yield 100%). ^1H NMR (500 MHz, DMSO- d_6): δ 1.26–1.38 (m, 1H), 1.37–1.49 (m, 1H), 1.53–1.65 (m, 1H), 1.70–1.83 (m, 1H), 1.99 (t_{br} , $J = 9.5$ Hz, 1H), 2.12 (t_{br} , $J = 9.8$ Hz, 1H), 2.38 (tt, $J = 9.9/3.9$ Hz, 1H), 2.42 (t, $J = 6.8$ Hz, 2H), 2.56–2.67 (m, 1H), 2.81 (d_{br} , $J = 10.6$ Hz, 1H), 3.11 (t, $J = 6.6$ Hz, 2H), 7.14–7.25 (s_{br} , 1H), 7.20 (dd, $J = 7.6/1.2$ Hz, 1H), 7.25–7.35 (m, 5H), 7.35–7.40 (m, 1H), 7.43–7.52 (m, 1H), 7.87 (dd, $J = 7.9/1.2$ Hz, 1H) ppm. ^{13}C NMR (101 MHz,

DMSO- d_6): δ 23.9, 26.4, 41.0, 45.4, 53.2, 55.3, 56.3, 115.5 (d, $^2J_{CF}$ = 22.1 Hz), 123.7, 124.5 (d, $^3/4J_{CF}$ = 3.6 Hz), 126.8, 127.2 (d, $^2J_{CF}$ = 16.3 Hz), 127.9, 129.7 (d, $^3J_{CF}$ = 8.1 Hz), 130.4, 131.5, 131.8 (d, $^3/4J_{CF}$ = 3.3 Hz), 132.8, 134.4, 158.9 (d, $^1J_{CF}$ = 244.3 Hz), 175.0 ppm. ^{19}F NMR (471 MHz, DMSO- d_6): δ -115.00 ppm. MS (ESI+) m/z : 370 [M + H] $^+$. HRMS (ESI+): [M + H] $^+$ calcd for C₂₁H₂₅O₂N₃F, 370.1931; found, 370.1923.

(E)-1-(2-{2-[1-(4'-Fluorobiphenyl-2-yl)methylidene]hydrazinyl}ethyl)piperidine-3-carboxylic Acid (12e). According to GPI from hydrazine **10** (8.55 mg, 45.6 μ mol) and **11e** (9.13 mg, 45.6 μ mol), **12e** was obtained as slightly yellow, amorphous solid (16.9 mg, yield 100%). 1H NMR (400 MHz, DMSO- d_6): δ 1.26–1.40 (m, 1H), 1.38–1.50 (m, 1H), 1.54–1.66 (m, 1H), 1.71–1.83 (m, 1H), 2.02 (t_{br}, J = 10.0 Hz, 1H), 2.15 (t_{br}, J = 10.2 Hz, 1H), 2.39 (tt, J = 8.9/3.9 Hz, 1H), 2.45 (t, J = 6.7 Hz, 2H), 2.56–2.69 (m, 1H), 2.82 (d_{br}, J = 10.3 Hz, 1H), 3.13 (t, J = 6.6 Hz, 2H), 7.01–7.18 (s_{br}, 1H), 7.17–7.23 (m, 1H), 7.24–7.31 (m, 3H), 7.31–7.39 (m, 3H), 7.43 (s, 1H), 7.85 (dd, J = 7.7/1.3 Hz, 1H) ppm. ^{13}C NMR (101 MHz, DMSO- d_6): δ 23.9, 26.4, 41.0, 45.5, 53.2, 55.3, 56.4, 115.1 (d, $^2J_{CF}$ = 21.0 Hz, 2C), 124.2, 126.9, 127.4, 130.0, 131.3 (d, $^3J_{CF}$ = 8.0 Hz, 2C), 132.0, 133.6, 136.2 (d, $^4J_{CF}$ = 3.3 Hz), 138.2, 161.4 (s, $^1J_{CF}$ = 240.7 Hz), 175.0 ppm. ^{19}F NMR (471 MHz, DMSO- d_6): δ -115.42 ppm. MS (ESI+) m/z : 370 [M + H] $^+$. HRMS (ESI+): [M + H] $^+$ calcd for C₂₁H₂₅O₂N₃F, 370.1931; found, 370.1923.

(E)-1-(2-{2-[1-(3',4'-Difluorobiphenyl-2-yl)methylidene]hydrazinyl}ethyl)piperidine-3-carboxylic Acid (12f). According to GPI from hydrazine **10** (10.2 mg, 54.5 μ mol) and **11f** (11.9 mg, 54.5 μ mol), **12f** was obtained as a yellow, amorphous solid (21.1 mg, yield 100%). 1H NMR (500 MHz, DMSO- d_6): δ 1.26–1.39 (m, 1H), 1.38–1.50 (m, 1H), 1.55–1.65 (m, 1H), 1.71–1.83 (m, 1H), 2.01 (t_{br}, J = 9.5 Hz, 1H), 2.14 (t_{br}, J = 9.9 Hz, 1H), 2.39 (tt, J = 9.9/3.9 Hz, 1H), 2.45 (t, J = 6.7 Hz, 2H), 2.58–2.68 (m, 1H), 2.84 (d_{br}, J = 9.7 Hz, 1H), 3.15 (t, J = 6.6 Hz, 2H), 7.13–7.18 (m, 1H), 7.19–7.26 (s_{br}, 1H), 7.23 (dd, J = 7.6/1.3 Hz, 1H), 7.29 (td, J = 7.4/1.4 Hz, 1H), 7.35 (td, J = 7.7/1.1 Hz, 1H), 7.39–7.46 (m, 1H), 7.44 (s, 1H), 7.52 (dt, J = 10.8/8.5 Hz, 1H), 7.85 (dd, J = 7.8/1.0 Hz, 1H) ppm. ^{13}C NMR (101 MHz, DMSO- d_6): δ 23.9, 26.5, 40.9, 45.4, 53.2, 55.3, 56.4, 117.3 (d, $^2J_{CF}$ = 16.9 Hz), 118.4 (d, $^2J_{CF}$ = 16.9 Hz), 124.2, 126.4 (d, J_{CF} = 6.4/3.4 Hz), 126.9, 127.8, 130.0, 131.5, 133.6, 137.1 (d, J_{CF} = 1.4 Hz), 137.4 (dd, J_{CF} = 6.1/3.8 Hz), 148.9 (d, $^{1/2}J_{CF}$ = 245.7/12.8 Hz), 149.0 (d, $^{1/2}J_{CF}$ = 245.7/12.8 Hz), 175.1 ppm. ^{19}F NMR (471 MHz, DMSO- d_6): δ -140.87 (m, 1 F), -138.46 (m, 1 F) ppm. MS (ESI+) m/z : 388 [M + H] $^+$. HRMS (ESI+): [M + H] $^+$ calcd for C₂₁H₂₄O₂N₃F₂, 388.1837; found, 388.1828.

(E)-1-(2-{2-[1-(2',4'-Difluorobiphenyl-2-yl)methylidene]hydrazinyl}ethyl)piperidine-3-carboxylic Acid (12g). According to GPI from hydrazine **10** (10.8 mg, 57.9 μ mol) and **11g** (12.6 mg, 57.9 μ mol), **12g** was obtained as a yellow, amorphous solid (22.6 mg, yield 100%). 1H NMR (400 MHz, DMSO- d_6): δ 1.25–1.51 (m, 2H), 1.53–1.66 (m, 1H), 1.70–1.83 (m, 1H), 1.99 (t_{br}, J = 10.4 Hz, 1H), 2.12 (t_{br}, J = 10.6 Hz, 1H), 2.30–2.48 (m, 3H), 2.62 (d_{br}, J = 11.8 Hz, 1H), 2.82 (d_{br}, J = 9.7 Hz, 1H), 3.12 (t, J = 6.4 Hz, 2H), 7.12–7.25 (m, 3H), 7.25–7.33 (m, 2H), 7.33–7.45 (m, 3H), 7.86 (d, J = 7.9 Hz, 1H) ppm. ^{13}C NMR (126 MHz, DMSO- d_6): δ 23.9, 26.4, 40.9, 45.4, 53.2, 55.3, 56.3, 103.9 (t, $^2J_{CF}$ = 26.2 Hz), 111.6 (dd, $^{2/4}J_{CF}$ = 21.3/3.4 Hz), 123.8, (dd, $^{2/4}J_{CF}$ = 15.6/3.5 Hz) 123.8, 126.8, 128.1, 130.5, 131.2, 131.9, 132.8 (dd, $^{3/3}J_{CF}$ = 9.6/4.8 Hz), 134.5, 159.0 (dd, $^{1/3}J_{CF}$ = 246.6/12.4 Hz), 161.8 (dd, $^{1/3}J_{CF}$ = 246.6/11.9 Hz), 175.1 ppm. ^{19}F NMR (471 MHz, DMSO- d_6): δ -110.87 (dt, J = 16.0/8.2 Hz), -110.40 (q, J = 8.0 Hz) ppm. MS (ESI+) m/z : 388.2 [M + H] $^+$. HRMS (ESI+): [M + H] $^+$ calcd for C₂₁H₂₄F₂N₃O₂, 388.1837; found, 388.1829.

(E)-1-(2-{2-[1-(2',3'-Difluorobiphenyl-2-yl)methylidene]hydrazinyl}ethyl)piperidine-3-carboxylic Acid (12h). According to GPI from hydrazine **10** (8.78 mg, 46.9 μ mol) and **11h** (10.2 mg, 46.9 μ mol), **12h** was obtained as a yellow, amorphous solid (18.0 mg, yield 99%). 1H NMR (500 MHz, DMSO- d_6): δ 1.25–1.38 (m, 1H), 1.38–1.50 (m, 1H), 1.54–1.65 (m, 1H), 1.71–1.83 (m, 1H), 1.99 (t_{br}, J = 9.6 Hz, 1H), 2.12 (t_{br}, J = 9.7 Hz, 1H), 2.38 (tt, J = 9.8/3.7 Hz, 1H), 2.42 (t, J = 6.7 Hz, 2H), 2.57–2.67 (m, 1H), 2.81 (d_{br}, J = 10.4

Hz, 1H), 3.12 (t, J = 6.6 Hz, 2H), 7.10–7.18 (m, 1H), 7.19–7.27 (m, 2H), 7.27–7.34 (m, 3H), 7.37–7.44 (m, 1H), 7.44–7.52 (m, 1H), 7.84–7.89 (m, 1H) ppm. ^{13}C NMR (126 MHz, DMSO- d_6): δ 23.9, 26.4, 40.9, 45.5, 53.2, 55.3, 56.4, 116.7 (d, $^2J_{CF}$ = 17.1 Hz), 123.9, 124.8 (dd, $^3/4J_{CF}$ = 7.5/4.6 Hz), 126.8, 127.0 (m_{CF}), 128.4, 129.7 (d, $^2J_{CF}$ = 12.8 Hz), 130.3, 131.0, 131.3 (s, $^3J_{CF}$ = 2.5 Hz), 134.4, 146.8 (dd, $^{1/2}J_{CF}$ = 246.4/12.7 Hz), 149.7 (dd, $^{1/2}J_{CF}$ = 246.3/13.1 Hz), 175.0 ppm. ^{19}F NMR (471 MHz, DMSO- d_6): δ -140.82 (d, J = 23.21 Hz), -138.54 (d, J = 27.07 Hz) ppm. MS (ESI+) m/z : 388.7 [M + H] $^+$. HRMS (ESI+): [M + H] $^+$ calcd for C₂₁H₂₄F₂N₃O₂, 388.1837; found, 388.1828.

(E)-1-(2-{2-[1-(4'-Fluoro-2'-methoxybiphenyl-2-yl)methylidene]hydrazinyl}ethyl)piperidine-3-carboxylic Acid (12i). According to GPI from hydrazine **10** (13.2 mg, 70.3 μ mol) and **11i** (16.2 mg, 70.3 μ mol), **12i** was obtained as colorless, amorphous solid (28.1 mg, yield 99%). 1H NMR (500 MHz, DMSO- d_6): δ 1.27–1.38 (m, 1H), 1.38–1.50 (m, 1H), 1.53–1.65 (m, 1H), 1.69–1.83 (m, 1H), 2.00 (t_{br}, J = 10.4 Hz, 1H), 2.14 (t_{br}, J = 9.8 Hz, 1H), 2.38 (tt, J = 9.7/3.9 Hz, 1H), 2.42 (t, J = 7.0 Hz, 2H), 2.56–2.67 (m, 1H), 2.81 (d_{br}, J = 11.3 Hz, 1H), 3.09 (t, J = 6.7 Hz, 2H), 3.71 (s, 3H), 6.84 (td, J = 8.4/2.5 Hz, 1H), 7.01 (dd, J = 11.5/2.4 Hz, 1H), 7.08 (dd, J = 7.6/1.3 Hz, 1H), 7.13 (dd, J = 8.3/7.0 Hz, 1H), 7.19 (s, 1H), 7.23 (td, J = 7.4/1.5 Hz, 1H), 7.26–7.33 (m, 1H), 7.81 (dd, J = 7.9/1.2 Hz, 1H) ppm. ^{13}C NMR (126 MHz, DMSO- d_6): δ 23.9, 26.4, 40.9, 45.5, 53.2, 55.3, 55.7, 56.4, 99.5 (d, $^2J_{CF}$ = 25.7 Hz), 106.6 (d, $^2J_{CF}$ = 21.0 Hz), 123.3, 124.8 (d, $^4J_{CF}$ = 2.8 Hz), 126.6, 127.2, 130.5, 131.8 (d, $^3J_{CF}$ = 10.0 Hz), 132.7, 134.4, 135.3, 157.5 (d, $^3J_{CF}$ = 10.2 Hz), 162.6 (d, $^1J_{CF}$ = 243.5 Hz), 175.1 ppm. ^{19}F NMR (471 MHz, DMSO- d_6): δ 111.80 (ddd, J = 11.4/8.4/7.2 Hz) ppm. MS (CI, CH₅ $^+$) m/z : 400 [M + H] $^+$. HRMS (ESI+): [M + H] $^+$ calcd for C₂₂H₂₇N₃O₃F, 400.2036; found, 400.2029.

(E)-1-(2-{2-[1-(2'-Fluoro-6'-methoxybiphenyl-2-yl)methylidene]hydrazinyl}ethyl)piperidine-3-carboxylic Acid (12m). According to GPI from hydrazine **10** (4.72 mg, 25.5 μ mol) and **11m** (5.80 mg, 25.2 μ mol), **12m** was obtained as a yellow, amorphous solid (10.8 mg, yield 100%). 1H NMR (500 MHz, DMSO- d_6): δ 1.25–1.36 (m, 1H), 1.35–1.48 (m, 1H), 1.52–1.64 (m, 1H), 1.70–1.81 (m, 1H), 1.96 (t_{br}, J = 9.9 Hz, 1H), 2.09 (t_{br}, J = 9.1 Hz, 1H), 2.32–2.39 (m, 1H), 2.39 (t, J = 6.7 Hz, 2H), 2.55–2.65 (m, 1H), 2.79 (d_{br}, J = 9.7 Hz, 1H), 3.07 (t, J = 6.6 Hz, 2H), 3.70 (s, 3H), 6.90 (t, J = 8.6 Hz, 1H), 6.97 (d, J = 8.5 Hz, 1H), 7.06–7.14 (s_{br}, 1H), 7.09 (dd, J = 7.6/1.0 Hz, 1H), 7.15 (s, 1H), 7.24 (td, J = 7.5/1.4 Hz, 1H), 7.31 (td, J = 7.7/1.0 Hz, 1H), 7.41 (td, J = 8.4/7.1 Hz, 1H), 7.83 (d, J = 7.9 Hz, 1H) ppm. ^{13}C NMR (101 MHz, DMSO- d_6): δ 23.9, 26.4, 40.9, 45.4, 53.2, 55.3, 55.9, 56.3, 107.3, 107.6 (d, 1 C, $^2J_{CF}$ = 22.9 Hz), 116.0 (d, $^2J_{CF}$ = 19.41 Hz), 123.4, 126.5, 127.7, 128.9, 129.8 (d, 1 C, $^3J_{CF}$ = 19.4 Hz), 131.0, 131.9, 134.9, 157.7 (d, $^3J_{CF}$ = 7.3 Hz), 159.5 (d, $^1J_{CF}$ = 241.6 Hz), 175.0 ppm. ^{19}F NMR (471 MHz, DMSO- d_6): δ -113.70 (t, J = 7.8 Hz) ppm. MS (ESI+) m/z : 400 [M + H] $^+$. HRMS (ESI+): [M + H] $^+$ calcd for C₂₂H₂₇O₃N₃F, 400.2036; found, 400.2028.

(E)-1-(2-{2-[1-(2'-Chlorobiphenyl-2-yl)methylidene]hydrazinyl}ethyl)piperidine-3-carboxylic Acid (12p). According to GPI from hydrazine **10** (12.7 mg, 68.1 μ mol) and **11p** (14.8 mg, 68.4 μ mol), **12p** was obtained as a yellow, amorphous solid (26.3 mg, yield 100%). 1H NMR (500 MHz, DMSO- d_6): δ 1.26–1.37 (m, 1H), 1.37–1.48 (m, 1H), 1.54–1.63 (m, 1H), 1.69–1.82 (m, 1H), 1.97 (t_{br}, J = 9.9 Hz, 1H), 2.04–2.19 (m, 1H), 2.32–2.44 (m, 3H), 2.60 (d_{br}, J = 10.5 Hz, 1H), 2.80 (d_{br}, J = 10.8 Hz, 1H), 3.08 (t, J = 6.6 Hz, 2H), 7.09–7.13 (m, 1H), 7.12 (s, 1H), 7.18 (s_{br}, 1H), 7.25–7.33 (m, 2H), 7.33–7.39 (m, 1H), 7.40–7.47 (m, 2H), 7.53–7.61 (m, 1H), 7.86 (dd, J = 8.0/0.7 Hz, 1H) ppm. ^{13}C NMR (126 MHz, DMSO- d_6): δ 23.9, 26.4, 40.9, 45.3, 53.2, 55.3, 56.2, 123.5, 126.6, 127.2, 127.9, 129.2, 129.3, 129.8, 131.1, 131.7, 132.4, 134.1, 136.5, 138.6, 175.0 ppm. MS (ESI+) m/z : 386 [M + H] $^+$. HRMS (ESI+): [M + H] $^+$ calcd for C₂₁H₂₅ClN₃O₂, 386.1635; found, 368.1629.

(E)-1-(2-{2-[1-(4'-Chlorobiphenyl-2-yl)methylidene]hydrazinyl}ethyl)piperidine-3-carboxylic Acid (12r). According to GPI from hydrazine **10** (9.65 mg, 51.6 μ mol) and **11r** (11.1 mg, 51.6 μ mol), **12r** was obtained as a yellow, amorphous solid (20.0 mg, yield 100%). 1H NMR (500 MHz, DMSO- d_6): δ 1.28–1.39 (m, 1H),

1.39–1.50 (m, 1H), 1.55–1.66 (m, 1H), 1.69–1.84 (m, 1H), 2.02 (t_{br}, J = 9.6 Hz, 1H), 2.15 (t_{br}, J = 10.0 Hz, 1H), 2.39 (tt, J = 9.9/3.8 Hz, 1H), 2.45 (t, J = 6.7 Hz, 2H), 2.58–2.67 (m, 1H), 2.83 (d_{br}, J = 11.6 Hz, 1H), 3.14 (t, J = 6.6 Hz, 2H), 7.20 (s_{br}, 1H), 7.21 (dd, J = 7.6/1.3 Hz, 1H), 7.29 (td, J = 7.4/1.5 Hz, 1H), 7.31–7.37 (m, 3H), 7.43 (s, 1H), 7.49–7.54 (m, 2H), 7.85 (dd, J = 7.8/1.3 Hz, 1H) ppm. ¹³C NMR (126 MHz, DMSO-*d*₆): δ 23.9, 26.4, 40.9, 45.5, 53.2, 55.3, 56.4, 124.3, 126.9, 127.6, 128.2 (2C), 129.8, 131.2 (2C), 131.8, 132.0, 133.5, 137.9, 138.7, 175.0 ppm. MS (ESI+) *m/z*: 386.1 [M + H]⁺. HRMS (ESI+): [M + H]⁺ calcd for C₂₁H₂₅ClN₃O₂, 386.1635; found, 386.1629.

(E)-1-(2-{2-[1-(4'-Methylbiphenyl-2-yl)methylidene]hydrazinyl}ethyl)piperidine-3-carboxylic Acid (12v). According to GPI from hydrazine **10** (11.1 mg, 59.5 μmol) and **11v** (11.7, 59.5 μmol), **12v** was obtained as colorless, amorphous solid (21.6 mg, yield 100%). ¹H NMR (500 MHz, DMSO-*d*₆): δ 1.26–1.39 (m, 1H), 1.39–1.51 (m, 1H), 1.53–1.66 (m, 1H), 1.69–1.84 (m, 1H), 2.01 (t_{br}, J = 10.2 Hz, 1H), 2.15 (t_{br}, J = 10.3 Hz, 1H), 2.36 (s, 3H), 2.39 (tt, J = 9.9/2.8 Hz, 1H), 2.45 (t, J = 6.5 Hz, 2H), 2.58–2.67 (m, 1H), 2.82 (d_{br}, J = 9.5 Hz, 1H), 3.13 (t, J = 6.7 Hz, 2H), 7.08 (s, 1H), 7.15–7.23 (m, 3H), 7.23–7.34 (m, 4H), 7.47 (s, 1H), 7.78–7.87 (m, 1H) ppm. ¹³C NMR (126 MHz, DMSO-*d*₆): δ 20.6, 23.9, 26.4, 40.9, 45.5, 53.2, 55.3, 56.4, 124.2, 126.9, 127.1, 128.8 (2C), 129.2 (2C), 129.9, 132.5, 133.4, 136.2, 136.9, 139.3, 175.0 ppm. MS (ESI+) *m/z*: 366.2 [M + H]⁺. HRMS (ESI+): [M + H]⁺ calcd for C₂₂H₂₈N₃O₂, 366.2182; found, 366.2174.

(E)-1-(2-{2-[1-(4'-Chloro-2'-fluorobiphenyl-2-yl)methylidene]hydrazinyl}ethyl)piperidine-3-carboxylic Acid (12y). According to GPI from hydrazine **10** (9.40 mg, 50.2 μmol) and **11y** (11.8 mg, 50.3 μmol), **12y** was obtained as a yellow, amorphous solid (20.3 mg, yield 100%). ¹H NMR (500 MHz, DMSO-*d*₆): δ 1.28–1.39 (m, 1H), 1.38–1.50 (m, 1H), 1.54–1.66 (m, 1H), 1.71–1.84 (m, 1H), 2.00 (t_{br}, J = 9.9 Hz, 1H), 2.14 (t_{br}, J = 10.1 Hz, 1H), 2.39 (tt, J = 9.8/3.8 Hz, 1H), 2.43 (t, J = 6.8 Hz, 2H), 2.57–2.68 (m, 1H), 2.82 (d_{br}, J = 9.2 Hz, 1H), 3.12 (t, J = 6.6 Hz, 2H), 7.14–7.25 (s_{br}, 1H), 7.19 (dd, J = 7.7/1.1 Hz, 1H), 7.27–7.29 (m, 1H), 7.30 (dd, J = 7.4/1.3 Hz, 1H), 7.33–7.43 (m, 3H), 7.53 (dd, J = 9.7/1.9 Hz, 1H), 7.85 (dd, J = 8.0/1.0 Hz, 1H) ppm. ¹³C NMR (126 MHz, DMSO-*d*₆): δ 23.9, 26.4, 40.9, 45.5, 53.2, 55.3, 56.3, 116.1 (d, ²J_{CF} = 26.3 Hz), 123.9, 124.8 (d, ⁴J_{CF} = 3.7 Hz), 126.4 (d, ²J_{CF} = 16.4 Hz), 126.8, 128.3, 130.3, 131.2, 131.6, 133.0 (d, ³J_{CF} = 4.0 Hz), 133.1 (d, ³J_{CF} = 10.4 Hz), 134.4, 158.9 (d, ¹J_{CF} = 248.0 Hz), 175.0 ppm. ¹⁹F NMR (471 MHz, DMSO-*d*₆): δ -111.84 (m) ppm. MS (ESI+) *m/z*: 404.2 [M + H]⁺. HRMS (ESI+): [M + H]⁺ calcd for C₂₁H₂₄ClFN₃O₂, 404.1541; found, 404.1534.

(E)-1-(2-{2-[1-(2',4'-Dichlorobiphenyl-2-yl)methylidene]hydrazinyl}ethyl)piperidine-3-carboxylic Acid (12z). According to GPI from hydrazine **10** (18.2 mg, 97.0 μmol) and **11z** (24.4 mg, 97.0 μmol), **12z** was obtained as a yellow, amorphous solid (40.6 mg, yield 99%). ¹H NMR (500 MHz, DMSO-*d*₆, 60 °C): δ 1.28–1.50 (m, 2H), 1.56–1.66 (m, 1H), 1.72–1.83 (m, 1H), 2.02 (t, J = 9.1 Hz, 1H), 2.16 (t, J = 10.3 Hz, 1H), 2.34–2.46 (m, 3H), 2.55–2.64 (m, 1H), 2.80 (dd, J = 11.1/3.3 Hz, 1H), 3.10 (t, J = 6.7 Hz, 2H), 7.10 (dd, J = 7.6/1.0 Hz, 1H), 7.16 (s, 1H), 7.28 (td, J = 7.5/1.4 Hz, 1H), 7.32 (d, J = 8.2 Hz, 1H), 7.34–7.39 (m, 1H), 7.48 (dd, J = 8.2/2.1 Hz, 1H), 7.68 (d, J = 2.1 Hz, 1H), 7.83 (dd, J = 8.0/1.2 Hz, 1H) ppm. ¹³C NMR (126 MHz, DMSO-*d*₆, 60 °C): δ 23.9, 26.5, 41.1, 45.7, 53.2, 55.4, 56.4, 124.0, 126.6, 127.3, 128.1, 128.7, 129.7, 131.3, 132.9, 133.0, 133.6, 134.4, 135.4, 138.0, 174.9 ppm. ¹⁹F NMR (471 MHz, DMSO-*d*₆): δ -111.84 (m) ppm. MS (ESI+) *m/z*: 420 [M + H]⁺. HRMS (ESI+): [M + H]⁺ calcd for C₂₁H₂₄N₃O₂Cl₂, 420.1246; found, 420.1210.

(E)-1-(2-{2-[1-(2',6'-Difluorobiphenyl-2-yl)methylidene]hydrazinyl}ethyl)piperidine-3-carboxylic Acid (12aa). According to GPI from hydrazine **10** (6.51 mg, 34.7 μmol) and **11aa** (7.57 mg, 34.7 μmol), **12aa** was obtained as a yellow, amorphous solid (13.3 mg, yield 99%). ¹H NMR (500 MHz, DMSO-*d*₆): δ 1.26–1.50 (m, 2H), 1.53–1.65 (m, 1H), 1.70–1.83 (m, 1H), 1.99 (t_{br}, J = 9.4 Hz, 1H), 2.13 (t_{br}, J = 10.1 Hz, 1H), 2.33–2.45 (m, 3H), 2.56–2.66 (m, 1H), 2.81 (d_{br}, J = 9.7 Hz, 1H), 3.10 (t, J = 6.7 Hz, 2H), 7.14–7.27 (m, 5H), 7.31 (td, J = 7.5/1.3 Hz, 1H), 7.41 (td, J = 7.7/1.0 Hz, 1H), 7.52

(tt, J = 8.4/6.6 Hz, 1H), 7.87 (dd, J = 8.0/1.0 Hz, 1H) ppm. ¹³C NMR (126 MHz, DMSO-*d*₆): δ 23.9, 26.4, 40.9, 45.4, 53.2, 55.3, 56.3, 111.7 (d, ²J_{CF} = 25.8 Hz, 2C), 116.3 (t, ²J_{CF} = 21.8 Hz), 124.1, 125.8, 126.7, 128.6, 130.3 (t, ³J_{CF} = 10.4 Hz), 130.8, 130.9, 135.1, 159.4 (d, ¹J_{CF} = 245.4 Hz, 2C), 175.0 ppm. ¹⁹F NMR (471 MHz, DMSO-*d*₆): δ -112.40 (t, J = 6.5 Hz) ppm. MS (ESI+) *m/z*: 388.3 [M + H]⁺. HRMS (ESI+): [M + H]⁺ calcd for C₂₁H₂₄N₃O₂F₂, 388.1837; found, 388.1834.

(E)-1-(2-{2-[1-(2',4',6'-Trifluorobiphenyl-2-yl)methylidene]hydrazinyl}ethyl)piperidine-3-carboxylic Acid (12ab). According to GPI from hydrazine **10** (10.9 mg, 58.4 μmol) and **11ab** (13.8 mg, 58.4 μmol), **12ab** was obtained as a yellow, amorphous solid (24.5 mg, yield 100%). ¹H NMR (500 MHz, DMSO-*d*₆): δ 1.27–1.39 (m, 1H), 1.38–1.50 (m, 1H), 1.53–1.66 (m, 1H), 1.68–1.85 (m, 1H), 1.99 (t_{br}, J = 9.8 Hz, 1H), 2.13 (t_{br}, J = 10.2 Hz, 1H), 2.34–2.45 (m, 3H), 2.55–2.69 (m, 1H), 2.82 (d_{br}, J = 10.7 Hz, 1H), 3.11 (t, J = 6.4 Hz, 2H), 7.22 (dd, J = 7.6/0.9 Hz, 1H), 7.19–7.28 (s_{br}, 1H), 7.27 (s, 1H), 7.29–7.36 (m, 3H), 7.38–7.46 (m, 1H), 7.81–7.87 (m, 1H) ppm. ¹³C NMR (126 MHz, DMSO-*d*₆): δ 23.9, 26.4, 40.9, 45.5, 53.2, 55.3, 56.3, 100.7 (t, ²J_{CF} = 28.0 Hz, 2C), 113.2 (td, ²/⁴J_{CF} = 22.2/4.8 Hz), 124.4, 124.9, 126.8, 128.8, 130.9, 131.0, 135.2, 159.6 (ddd, J_{CF} = 246.1/15.5/10.1 Hz, 2C), 161.7 (dt, J_{CF} = 246.1/15.9 Hz), 175.0 ppm. ¹⁹F NMR (471 MHz, DMSO-*d*₆): δ -109.39 (t, J = 6.8 Hz), -108.58 (tt, J = 9.3/6.4 Hz) ppm. MS (ESI+) *m/z*: 406.0 [M + H]⁺. HRMS (ESI+): [M + H]⁺ calcd for C₂₁H₂₃F₃N₃O₂, 406.1742; found, 406.1735.

(E)-1-(2-{2-[1-(4,2'-Difluorobiphenyl-2-yl)methylidene]hydrazinyl}ethyl)piperidine-3-carboxylic Acid (12ac). According to GPI from hydrazine **10** (9.55 mg, 51.0 μmol) and **11ac** (11.1 mg, 51.0 μmol), **12ac** was obtained as a yellow, amorphous solid (21.0 mg, yield 100%). ¹H NMR (500 MHz, DMSO-*d*₆): δ 1.26–1.38 (m, 1H), 1.38–1.49 (m, 1H), 1.53–1.65 (m, 1H), 1.70–1.84 (m, 1H), 1.99 (t_{br}, J = 9.5 Hz, 1H), 2.12 (t_{br}, J = 10.0 Hz, 1H), 2.38 (tt, J = 9.9/3.8 Hz, 1H), 2.43 (t, J = 6.7 Hz, 2H), 2.58–2.66 (m, 1H), 2.81 (d, J = 9.8 Hz, 1H), 3.13 (t_{br}, J = 6.2 Hz, 2H), 7.11 (td, J = 8.4/2.8 Hz, 1H), 7.20 (t, J = 2.3 Hz, 1H), 7.25 (dd, J = 8.5/5.9 Hz, 1H), 7.28–7.35 (m, 3H), 7.43–7.51 (m, 2H), 7.56 (dd, J = 10.8/2.8 Hz, 1H) ppm. ¹³C NMR (126 MHz, DMSO-*d*₆): δ 23.9, 26.4, 40.9, 45.3, 53.2, 55.3, 56.2, 109.2 (d, ²J_{CF} = 22.9 Hz), 113.6 (d, ²J_{CF} = 22.1 Hz), 115.5 (d, ²J_{CF} = 22.1 Hz), 124.6 (d, ⁴J_{CF} = 3.5 Hz), 126.3 (d, ²J_{CF} = 16.1 Hz), 128.8 (d, ⁴J_{CF} = 2.7 Hz), 129.4 (m_{CF}), 129.9 (d, ³J_{CF} = 8.1 Hz), 132.0 (d, ⁴J_{CF} = 3.2 Hz), 132.6 (d, ³J_{CF} = 8.5 Hz), 137.0 (d, ³J_{CF} = 9.0 Hz), 159.0 (s-d, ¹J_{CF} = 244.2 Hz), 162.0 (s-d, ¹J_{CF} = 244.0 Hz), 175.0 ppm. ¹⁹F NMR (471 MHz, DMSO-*d*₆): δ -115.08 to -114.96 (td, J = 7.1/3.5 Hz), -114.06 to -113.90 (m) ppm. MS (ESI+) *m/z*: 388.3 [M + H]⁺. HRMS (ESI+): [M + H]⁺ calcd for C₂₁H₂₄N₃O₂F₂, 388.1837; found, 388.1833.

(E)-1-(2-{2-[1-(2'-Chloro-4-fluorobiphenyl-2-yl)methylidene]hydrazinyl}ethyl)piperidine-3-carboxylic Acid (12ad). According to GPI from hydrazine **10** (7.17 mg, 38.3 μmol) and **11ad** (8.99 mg, 38.3 μmol), **12ad** was obtained as a yellow, amorphous solid (16.2 mg, yield 100%). ¹H NMR (500 MHz, DMSO-*d*₆): δ 1.26–1.37 (m, 1H), 1.37–1.47 (m, 1H), 1.54–1.63 (m, 1H), 1.70–1.82 (m, 1H), 1.97 (t_{br}, J = 10.2 Hz, 1H), 2.10 (t_{br}, J = 10.1 Hz, 1H), 2.32–2.44 (m, 3H), 2.56–2.63 (m, 1H), 2.79 (d_{br}, J = 9.2 Hz, 1H), 3.05–3.13 (m, 2H), 7.03 (d, J = 2.0 Hz, 1H), 7.10 (td, J = 8.4/2.8 Hz, 1H), 7.13–7.19 (m, 1H), 7.28–7.34 (m, 1H), 7.40–7.49 (m, 3H), 7.54 (dd, J = 10.8/2.7 Hz, 1H), 7.56–7.59 (m, 1H) ppm. ¹³C NMR (126 MHz, DMSO-*d*₆): δ 23.9, 26.4, 40.9, 45.2, 53.1, 55.3, 56.1, 108.9 (d, ²J_{CF} = 23.1 Hz), 113.3 (d, ²J_{CF} = 22.3 Hz), 127.2, 129.2 (m_{CF}), 129.3 (d, ⁴J_{CF} = 2.4 Hz), 129.5, 131.8, 132.0 (d, ³J_{CF} = 8.50 Hz), 132.5 (d, ⁴J_{CF} = 3.0 Hz), 132.6, 136.9 (d, 1 C, ³J_{CF} = 8.2 Hz), 137.7, 161.8 (d, ¹J_{CF} = 243.3 Hz), 175.0 ppm. ¹⁹F NMR (471 MHz, DMSO-*d*₆): δ -114.03 ppm. MS (ESI+) *m/z*: 404.3 [M + H]⁺. HRMS (ESI+): [M + H]⁺ calcd for C₂₁H₂₄N₃O₂F₂, 404.1541; found, 404.1538.

(E)-1-(2-{2-[1-(2'-Methylbiphenyl-2-yl)methylidene]hydrazinyl}ethyl)piperidine-3-carboxylic Acid (12ae). According to GPI from hydrazine **10** (10.3 mg, 58.4 μmol) and **11ae** (11.5 mg, 58.4 μmol), **12ae** was obtained as a yellow, amorphous solid (21.3 mg, yield 100%). ¹H NMR (500 MHz, DMSO-*d*₆): δ 1.26–1.37 (m, 1H), 1.36–1.47 (m, 1H), 1.53–1.63 (m, 1H), 1.71–1.81 (m, 1H), 1.93–

2.02 (m, 1H), 2.00 (s, 3H), 2.06–2.18 (m, 1H), 2.33–2.40 (m, 1H), 2.40 (t, $J = 6.7$ Hz, 2H), 2.55–2.63 (m, 1H), 2.74–2.84 (m, 1H), 3.07 (t, $J = 6.7$ Hz, 2H), 7.03–7.15 (m, 3H), 7.10 (s, 1H), 7.22–7.35 (m, 5H), 7.85 (dd, $J = 7.8/1.0$ Hz, 1H) ppm. ^{13}C NMR (126 MHz, DMSO- d_6): δ 19.7, 23.8, 26.4, 40.9, 45.4, 53.2, 55.3, 56.3, 123.4, 125.7, 126.7, 127.2, 127.4, 129.5, 129.7, 131.7, 133.8, 135.4, 138.9, 139.6, 175.0 ppm. MS (ESI+) m/z : 366.2 [M + H] $^+$. HRMS (ESI+): [M + H] $^+$ calcd for $\text{C}_{22}\text{H}_{28}\text{N}_3\text{O}_2$, 366.2182; found, 366.2175.

(E)-1-(2-[2-[1-(2',4'-Dimethylbiphenyl-2-yl)methylidene]hydrazinyl]ethyl)piperidine-3-carboxylic Acid (12af). According to GP1 from hydrazine **10** (17.6 mg, 94.1 μmol) and **11af** (19.7 mg, 94.1 μmol), **12af** was obtained as a yellow, amorphous solid (38.5 mg, yield 100%). ^1H NMR (500 MHz, DMSO- d_6 , 60 $^\circ\text{C}$): δ 1.29–1.40 (m, 1H), 1.38–1.49 (m, 1H), 1.53–1.65 (m, 1H), 1.69–1.82 (m, 1H), 1.96 (s, 3H), 1.98–2.05 (m, 1H), 2.12–2.20 (m, 1H), 2.32 (s, 3H), 2.33–2.44 (m, 3H), 2.54–2.62 (m, 1H), 2.74–2.82 (m, 1H), 3.08 (t, $J = 6.7$ Hz, 2H), 6.96 (d, $J = 7.6$ Hz, 1H), 7.01–7.08 (m, 2H), 7.10 (s, 1H), 7.13 (s, 1H), 7.24 (td, $J = 7.4/1.4$ Hz, 1H), 7.29 (td, $J = 7.4/0.9$ Hz, 1H), 7.83 (dd, $J = 7.8/1.1$ Hz, 1H) ppm. ^{13}C NMR (126 MHz, DMSO- d_6 , 60 $^\circ\text{C}$): δ 19.6, 20.6, 23.9, 26.5, 41.0, 45.7, 53.2, 55.3, 56.4, 123.6, 126.2, 126.7, 127.0, 129.5, 129.7, 130.4, 132.4, 134.2, 135.2, 136.4, 136.8, 139.1, 174.8 ppm. MS (ESI+) m/z : 380.5 [M + H] $^+$. HRMS (ESI+): [M + H] $^+$ calcd for $\text{C}_{23}\text{H}_{30}\text{N}_3\text{O}_2$, 379.2260; found, 380.2334.

(E)-1-(2-[2-[1-(2',4'-Bistrifluoromethylbiphenyl-2-yl)methylidene]hydrazinyl]ethyl)piperidine-3-carboxylic Acid (12ag). According to GP1 from hydrazine **10** (14.4 mg, 77.1 μmol) and **11ag** (24.5 mg, 77.1 μmol), **12ag** was obtained as a yellow, amorphous solid (35.1 mg, yield 93%). ^1H NMR (500 MHz, DMSO- d_6): δ 1.25–1.47 (m, 2H), 1.52–1.63 (m, 1H), 1.71–1.81 (m, 1H), 1.94 (t, $J = 10.5$ Hz, 1H), 2.02–2.15 (m, 1H), 2.25–2.41 (m, 3H), 2.53–2.60 (m, 1H), 2.71–2.84 (m, 1H), 3.03 (t, $J = 6.7$ Hz, 2H), 7.05 (s, 1H), 7.13 (d, $J = 7.6$ Hz, 1H), 7.13–7.23 (s_{br} , 1H), 7.22–7.31 (m, 1H), 7.37–7.44 (m, 1H), 7.56–7.63 (m, 1H), 7.81 (d, $J = 7.7$ Hz, 1H), 8.11 (d, $J = 8.1$ Hz, 1H), 8.15 (s, 1H) ppm. ^{13}C NMR (126 MHz, DMSO- d_6): δ 23.8, 26.4, 40.9, 45.5, 53.1, 55.3, 56.4, 122.9 (m_{CF}), 123.1 (q , $^1J_{\text{CF}} = 274.8$ Hz), 123.4 (q , $^1J_{\text{CF}} = 272.8$ Hz), 124.0, 126.0, 128.5, 128.7 (q , $^2J_{\text{CF}} = 32.8$ Hz), 128.8 (q , $^2J_{\text{CF}} = 32.2$ Hz), 128.9 (m_{CF}), 129.3, 131.1, 133.7, 134.1, 134.5, 143.8, 175.0 ppm. ^{19}F NMR (471 MHz, DMSO- d_6): δ -61.12 (m), -57.61 (d, $J = 2.5$ Hz) ppm. MS (ESI+) m/z : 488.3 [M + H] $^+$. HRMS (ESI+): [M + H] $^+$ calcd for $\text{C}_{23}\text{H}_{24}\text{F}_6\text{N}_3\text{O}_2$, 487.1694; found, 488.1768.

(E)-1-(2-[2-[1-(2'-Chloro-4'-fluorobiphenyl-2-yl)methylidene]hydrazinyl]ethyl)piperidine-3-carboxylic Acid (12ah). According to GP1 from hydrazine **10** (9.93 mg, 53.0 μmol) and **11ah** (12.4 mg, 53.0 μmol), **12ah** was obtained as a yellow, amorphous solid (21.3 mg, yield 100%). ^1H NMR (400 MHz, DMSO- d_6): δ 1.26–1.50 (m, 2H), 1.53–1.65 (m, 1H), 1.70–1.84 (m, 1H), 1.98 (t, $J = 10.2$ Hz, 1H), 2.12 (t, $J = 10.0$ Hz, 1H), 2.30–2.47 (m, 3H), 2.55–2.65 (m, 1H), 2.80 (d, $J = 10.6$ Hz, 1H), 3.09 (t, $J = 6.7$ Hz, 2H), 7.03–7.22 (m, 3H), 7.22–7.43 (m, 4H), 7.56 (dt, $J = 8.9/2.3$ Hz, 1H), 7.84 (d, $J = 7.9$ Hz, 1H) ppm. ^{13}C NMR (126 MHz, DMSO- d_6): δ 24.0, 26.5, 41.0, 45.5, 53.3, 55.4, 56.4, 114.5 (d, $^2J_{\text{CF}} = 21.3$ Hz), 116.5 (d, $^2J_{\text{CF}} = 24.7$ Hz), 123.7, 126.7, 128.1, 130.0, 131.2, 133.0 (d, $^3J_{\text{CF}} = 8.7$ Hz), 133.4 (d, $^3J_{\text{CF}} = 10.5$ Hz), 134.4, 135.3 (d, $^4J_{\text{CF}} = 3.6$ Hz), 135.6, 161.4 (d, $^1J_{\text{CF}} = 247.8$ Hz), 175.1 ppm. ^{19}F NMR (471 MHz, DMSO- d_6): δ -112.61 (tdd, $J = 8.8/6.3/2.4$ Hz) ppm. MS (ESI+) m/z : 404.3 [M + H] $^+$. HRMS (ESI+): [M + H] $^+$ calcd for $\text{C}_{21}\text{H}_{24}\text{ClFN}_3\text{O}_2$, 404.1541; found, 404.1537.

(E)-1-(2-[2-[1-(4'-Chloro-4-fluorobiphenyl-2-yl)methylidene]hydrazinyl]ethyl)piperidine-3-carboxylic Acid (12ak). According to GP1 from hydrazine **10** (8.91 mg, 47.6 μmol) and **11ak** (11.2 mg, 47.6 μmol), **12ak** was obtained as a yellow, amorphous solid (19.3 mg, yield 100%). ^1H NMR (400 MHz, DMSO- d_6): δ 1.24–1.42 (m, 1H), 1.37–1.51 (m, 1H), 1.53–1.67 (m, 1H), 1.70–1.84 (m, 1H), 2.00 (t, $J = 10.3$ Hz, 1H), 2.13 (t_{br} , $J = 10.3$ Hz, 1H), 2.38 (tt, $J = 9.8/3.7$ Hz, 1H), 2.44 (t, $J = 6.6$ Hz, 2H), 2.56–2.67 (m, 1H), 2.82 (d_{br} , $J = 10.7$ Hz, 1H), 3.15 (t, $J = 6.5$ Hz, 2H), 7.10 (td, $J = 8.4/2.8$ Hz, 1H), 7.25 (dd, $J = 8.5/5.9$ Hz, 1H), 7.29–7.37 (m, 3H), 7.38–7.48 (m, 1H), 7.48–7.54 (m, 2H), 7.52–7.56 (m, 1H) ppm. ^{13}C NMR (101 MHz,

DMSO- d_6): δ 23.9, 26.4, 41.0, 45.3, 53.2, 55.3, 56.3, 109.5 (d, $^2J_{\text{CF}} = 22.7$ Hz) 113.7 (d, $^2J_{\text{CF}} = 22.1$ Hz), 128.3 (2C), 129.7 (d, $^4J_{\text{CF}} = 2.7$ Hz), 131.3 (2C), 132.1 (d, $^3J_{\text{CF}} = 8.7$ Hz), 132.1, 134.1 (d, $^4J_{\text{CF}} = 2.5$ Hz), 136.2, 137.8, 161.7 (d, $^1J_{\text{CF}} = 244.3$ Hz), 175.0 ppm. ^{19}F NMR (471 MHz, DMSO- d_6): δ -114.45 (m) ppm. MS (ESI+) m/z : 404.2 [M + H] $^+$. HRMS (ESI+): [M + H] $^+$ calcd for $\text{C}_{21}\text{H}_{24}\text{ClFN}_3\text{O}_2$, 404.1541; found, 404.1539.

[(E)-5-(4,4,5,5-Tetramethyl-1,3,2-dioxaborolan-2-yl)pent-1-enyl]-4-methylbenzene Sulfonate (17). Chlorobis-(cyclopentadienyl)hydrido-zirconium (258 mg, 1.00 mmol) was added to a mixture of pent-4-enyl-4-methylbenzenesulfonate⁴³ (2.38 g, 10.0 mmol) and 4,4,5,5-tetramethyl-1,3,2-dioxaborolane (1.41 g, 11.0 mmol). The mixture was stirred at room temperature for 48 h and afterward diluted with CH_2Cl_2 . The solution was filtered through a short pad of silica gel (2 cm) and washed with CH_2Cl_2 . The filtrate was concentrated and dried in vacuo to give **17** as a colorless, high viscous liquid (3.48 g, 95%). ^1H NMR (400 MHz, CDCl_3): δ 1.24 (s, 12H), 1.75 (p, $J = 6.9$ Hz, 2H), 2.15 (q, $J = 6.9$ Hz, 2H), 2.44 (s, 3H), 4.01 (t, $J = 6.4$ Hz, 2H), 5.33 (dt, $J = 17.9/1.4$ Hz, 1H), 6.47 (dt, $J = 18.0/6.4$ Hz, 1H), 7.33 (dd, $J = 8.0/0.6$ Hz, 2H), 7.77 (d, $J = 8.4$ Hz, 2H) ppm. ^{13}C NMR (101 MHz, CDCl_3): δ 21.6, 24.7 (4C), 27.3, 31.3, 69.8, 83.1 (2C), 120.0,⁴⁷ 127.9 (2C), 129.8 (2C), 133.0, 144.7, 151.7 ppm. MS (ESI+) m/z : 367.1 [M + H] $^+$. HRMS (EI, 70 eV): M^+ calcd for $\text{C}_{18}\text{H}_{27}\text{BO}_2\text{S}$, 366.1672; found, 366.1670.

Ethyl 1-[(E)-5-(4,4,5,5-Tetramethyl-1,3,2-dioxaborolan-2-yl)pent-1-enyl]piperidine-3-carboxylate (18). Ethyl nipecotate (1.96 g, 12.5 mmol) was added to [(E)-5-(4,4,5,5-tetramethyl-1,3,2-dioxaborolan-2-yl)pent-4-enyl]-4-methylbenzene sulfonate (1.83 g, 5.00 mmol), and the mixture was stirred at room temperature for 16 h. Then water was added, and the aqueous phase was extracted with CH_2Cl_2 . The organic phase was washed with water and concentrated under reduced pressure. The residue was dissolved in Et_2O and filtered through a short pad of silica gel (3 cm). The filtrate was concentrated and dried in high vacuum to give **18** as a pale yellow liquid (1.62 g, 4.6 mmol, 92%). The product was used without further purification. ^1H NMR (400 MHz, CDCl_3): δ 1.19–1.26 (m, 15H), 1.33–1.45 (m, 1H), 1.46–1.64 (m, 3H), 1.68 (dp, $J = 10.4/3.5$ Hz, 1H), 1.84–1.97 (m, 2H), 2.01–2.17 (m, 3H), 2.23–2.34 (m, 2H), 2.51 (tt, $J = 10.6/3.7$ Hz, 1H), 2.72 (d, $J = 11.1$ Hz, 1H), 2.94 (d, $J = 10.1$ Hz, 1H), 4.09 (q, $J = 7.2$ Hz, 2H), 5.40 (d, $J = 18.0$ Hz, 1H), 6.60 (dt, $J = 17.9/6.4$ Hz, 1H) ppm. ^{13}C NMR (101 MHz, CDCl_3): δ 14.14, 24.53, 24.7 (4C), 25.3, 27.0, 33.6, 41.8, 53.7, 55.4, 58.2, 60.2, 82.9 (2C), 154.0, 174.2 ppm. MS (ESI+) m/z : 352 [M + H] $^+$. HRMS (EI, 70 eV): M^+ calcd for $\text{C}_{19}\text{H}_{34}\text{BNO}_4$, 351.2580; found, 351.2572.

Ethyl 1-[(E)-5-(2-Bromophenyl)pent-1-enyl]piperidine-3-carboxylate (19). Under nitrogen atmosphere $\text{Pd}(\text{dppf})\text{Cl}_2 \cdot \text{CH}_2\text{Cl}_2$ (41 mg, 0.025 mmol), 1-bromo-2-iodobenzene (312 mg, 1.10 mmol), and compound **18** (351 mg, 1.00 mmol) were dissolved in a mixture of 1,4-dioxane/water 2:1 (1.5 mL) and K_2CO_3 (414 mg, 3.00 mmol). The resulting mixture was stirred at room temperature for 72 h. After addition of water (5 mL) the mixture was extracted three times with CH_2Cl_2 (10 mL). The combined organic layers were dried over Na_2SO_4 and the solvent was removed in vacuo. The residue was purified by flash column chromatography on silica gel (n -pentane/ $\text{CH}_2\text{Cl}_2/\text{EtOAc} = 8/1/1 + 2\%$ Et_3N , $R_f = 0.3$) to give the **19** as a colorless oil (342 mg, 90%). ^1H NMR (400 MHz, CDCl_3): δ 1.25 (t, $J = 7.1$ Hz, 3H), 1.44 (qd, $J = 12.2/4.0$ Hz, 1H), 1.52–1.65 (m, 1H), 1.65–1.77 (m, 3H), 1.90–2.03 (m, 2H), 2.15 (t, $J = 10.6$ Hz, 1H), 2.27 (q, $J = 6.9$ Hz, 2H), 2.37–2.43 (m, 2H), 2.57 (tt, $J = 10.6/3.8$ Hz, 1H), 2.79 (d, $J = 11.0$ Hz, 1H), 3.01 (d, $J = 10.4$ Hz, 1H), 4.13 (q, $J = 7.1$ Hz, 2H), 6.16 (dt, $J = 15.6/6.9$ Hz, 1H), 6.71 (d, $J = 15.7$ Hz, 1H), 7.05 (td, $J = 7.9/1.5$ Hz, 1H), 7.24 (td, $J = 7.5/0.7$ Hz, 1H), 7.48 (dd, $J = 7.8/1.4$ Hz, 1H), 7.52 (dd, $J = 8.0/0.7$ Hz, 1H) ppm. ^{13}C NMR (101 MHz, CDCl_3): δ 14.2, 24.6, 26.3, 27.0, 30.9, 41.9, 53.8, 55.4, 58.2, 60.2, 123.1, 126.7, 127.3, 128.1, 128.9, 132.7, 133.5, 137.5, 174.2 ppm. MS (CI, CH_5^+) m/z : 381 [M + H] $^+$. HRMS (EI, 70 eV): M^+ calcd for $\text{C}_{19}\text{H}_{26}\text{BrNO}_2$, 379.1147; found, 379.1128.

Ethyl 1-[(E)-5-(2'-Fluorobiphenyl-2-yl)pent-4-en-1-yl]piperidine-3-carboxylate (21c). According to the GP2 from **19** (114 mg, 0.300 mmol) and **20c** (46 mg, 0.33 mmol), **21c** was obtained

as a slightly yellow oil (110 mg, 93%). ¹H NMR (500 MHz, CDCl₃): δ 1.24 (t, *J* = 7.1 Hz, 3H), 1.42 (qd, *J* = 11.9/3.6 Hz, 1H), 1.50–1.61 (m, 3H), 1.70 (dp, *J* = 13.0/3.7 Hz, 1H), 1.89–1.97 (m, 2H), 2.06–2.14 (m, 3H), 2.28–2.33 (m, 2H), 2.53 (tt, *J* = 10.7/3.8 Hz, 1H), 2.73 (d, *J* = 11.1 Hz, 1H), 2.95 (d, *J* = 10.0 Hz, 1H), 4.12 (q, *J* = 7.1 Hz, 2H), 6.13 (dt, *J* = 15.7/6.7 Hz, 1H), 6.21 (d, *J* = 16.0 Hz, 1H), 7.13 (ddd, *J* = 9.8/8.2/1.1 Hz, 1H), 7.18 (td, *J* = 7.4/1.1 Hz, 1H), 7.21–7.28 (m, 3H), 7.31–7.37 (m, 2H), 7.59 (d, *J* = 7.7 Hz, 1H) ppm. ¹³C NMR (126 MHz, CDCl₃): δ 14.2, 24.6, 26.4, 27.0, 31.0, 41.9, 53.8, 55.4, 58.2, 60.2, 115.5 (d, ²*J*_{CF} = 22.4 Hz), 123.8 (d, ⁴*J*_{CF} = 3.7 Hz), 125.3, 126.6, 128.0, 128.2, 128.5 (d, ²*J*_{CF} = 16.3 Hz), 129.1 (d, ³*J*_{CF} = 7.9 Hz), 130.5, 131.8, 132.1 (d, ³*J*_{CF} = 3.5 Hz), 134.0, 136.5, 159.6 (d, ¹*J*_{CF} = 246.6 Hz), 174.3 ppm. MS (CI, CH₅⁺) *m/z*: 396 [M + H]⁺. HRMS (EI, 70 eV): M⁺ calcd for C₂₅H₃₀FNO₂, 395.2261; found, 395.2265.

Ethyl 1-[(E)-5-(2',4'-Difluorobiphenyl-2-yl)pent-4-en-1-yl]piperidine-3-carboxylate (21g). According to GP2 from **19** (114 mg, 0.300 mmol) and **20g** (52 mg, 0.33 mmol), **21g** was obtained as a slightly yellow oil (113 mg, 91%). ¹H NMR (500 MHz, CDCl₃): δ 1.25 (t, *J* = 7.1 Hz, 3H), 1.42 (qd, *J* = 11.9/3.8 Hz, 1H), 1.49–1.64 (m, 3H), 1.71 (dp, *J* = 13.0/3.6 Hz, 1H), 1.89–1.97 (m, 2H), 2.05–2.16 (m, 3H), 2.28–2.35 (m, 2H), 2.54 (tt, *J* = 10.6/3.8 Hz, 1H), 2.74 (d, *J* = 10.6 Hz, 1H), 2.97 (d, *J* = 10.5 Hz, 1H), 4.12 (q, *J* = 7.1 Hz, 2H), 6.08–6.22 (m, 2H), 6.87–6.97 (m, 2H), 7.17–7.23 (m, 2H), 7.27 (td, *J* = 7.6/1.3 Hz, 1H), 7.35 (td, *J* = 7.6/1.2 Hz, 1H), 7.59 (d, *J* = 7.8 Hz, 1H) ppm. ¹³C NMR (126 MHz, CDCl₃): δ 14.2, 24.6, 26.4, 27.0, 31.0, 41.9, 53.8, 55.5, 58.2, 60.3, 103.9 (dd, ^{2/2}*J*_{CF} = 26.4/25.2 Hz), 111.0 (dd, ^{2/4}*J*_{CF} = 21.0/3.8 Hz), 124.61 (dd, ^{2/4}*J*_{CF} = 16.6/3.8 Hz), 125.5, 126.7, 128.0, 128.2, 130.6, 132.1, 132.7 (dd, ^{3/3}*J*_{CF} = 9.5/5.0 Hz), 133.0, 136.7, 159.6 (dd, ^{1/3}*J*_{CF} = 249.2/11.9 Hz), 162.4 (dd, ^{1/3}*J*_{CF} = 248.4/11.5 Hz), 174.3 ppm. MS (CI, CH₅⁺) *m/z*: 414 [M + H]⁺. HRMS (EI, 70 eV): M⁺ calcd for C₂₅H₂₉F₂NO₂, 413.2166; found, 413.2164.

Ethyl 1-[(E)-5-(2'-Chlorobiphenyl-2-yl)pent-4-en-1-yl]piperidine-3-carboxylate (21p). According to the GP2 from **19** (114 mg, 0.300 mmol) and **20p** (52 mg, 0.33 mmol), **21p** was obtained as a slightly yellow oil (115 mg, 93%). ¹H NMR (500 MHz, CDCl₃): δ 1.24 (t, *J* = 7.1 Hz, 3H), 1.40 (qd, *J* = 11.7/3.7 Hz, 1H), 1.48–1.59 (m, 3H), 1.70 (dp, *J* = 13.1/3.6 Hz, 1H), 1.90 (m, 2H), 2.02–2.11 (m, 3H), 2.25–2.31 (m, 2H), 2.52 (tt, *J* = 10.6/3.8 Hz, 1H), 2.72 (d, *J* = 11.1 Hz, 1H), 2.94 (d, *J* = 10.4 Hz, 1H), 4.11 (q, *J* = 7.1 Hz, 2H), 6.02–6.15 (m, 2H), 7.15 (d, *J* = 7.5 Hz, 1H), 7.21–7.31 (m, 4H), 7.34 (t, *J* = 7.6 Hz, 1H), 7.43–7.47 (m, 1H), 7.59 (d, *J* = 7.8 Hz, 1H) ppm. ¹³C NMR (101 MHz, CDCl₃): δ 14.2, 24.6, 26.4, 27.0, 31.0, 41.9, 53.8, 55.4, 58.2, 60.3, 125.0, 126.4 (2C), 128.0 (2C), 128.6, 129.4, 130.0, 131.6, 131.8, 133.5, 136.2, 137.6, 139.8, 174.3 ppm. MS (CI, CH₅⁺) *m/z*: 412 [M + H]⁺. HRMS (EI, 70 eV): M⁺ calcd for C₂₅H₃₀ClNO₂, 411.1965; found, 411.1966.

Ethyl 1-[(E)-5-(2',4'-Dichlorobiphenyl-2-yl)pent-4-en-1-yl]piperidine-3-carboxylate (21z). According to the GP2 from **19** (114 mg, 0.300 mmol) and **20z** (63 mg, 0.33 mmol), **21z** was obtained as a slightly yellow oil (123 mg, 92%). ¹H NMR (400 MHz, CDCl₃, 21 °C, TMS): δ 1.25 (t, *J* = 7.1 Hz, 3H), 1.42 (qd, *J* = 12.0/3.7 Hz, 1H), 1.49–1.62 (m, 3H), 1.71 (dp, *J* = 13.2/3.6 Hz, 1H), 1.89–1.97 (m, 2H), 2.05–2.13 (m, 3H), 2.27–2.32 (m, 2H), 2.53 (td, *J* = 10.6/5.3 Hz, 1H), 2.73 (d, *J* = 11.0 Hz, 1H), 2.96 (d, *J* = 10.6 Hz, 1H), 4.12 (q, *J* = 7.1 Hz, 2H), 6.03 (d, *J* = 15.8 Hz, 1H), 6.13 (dt, *J* = 15.7/6.7 Hz, 1H), 7.12 (dd, *J* = 7.5/1.0 Hz, 1H), 7.17 (d, *J* = 8.2 Hz, 1H), 7.24–7.31 (m, 2H), 7.36 (td, *J* = 7.7/1.0 Hz, 1H), 7.49 (t, *J* = 1.7 Hz, 1H), 7.59 (d, *J* = 7.8 Hz, 1H) ppm. ¹³C NMR (101 MHz, CDCl₃): δ 14.2, 24.6, 26.4, 27.0, 31.0, 41.9, 53.8, 55.4, 58.2, 60.3, 125.2, 126.6, 126.8, 127.6, 128.3, 129.2, 129.9, 132.2, 132.4, 133.7, 134.4, 136.3, 136.4, 138.5, 174.3 ppm. MS (CI, CH₅⁺) *m/z*: 446 [M + H]⁺. HRMS (EI, 70 eV): M⁺ calcd for C₂₅H₂₉Cl₂NO₂, 445.1575; found, 445.1549.

Ethyl 1-[(E)-5-(2'-Chloro-4'-fluorobiphenyl-2-yl)pent-4-en-1-yl]piperidine-3-carboxylate (21ah). According to the GP2 from **19** (114 mg, 0.300 mmol) and **20ah** (58 mg, 0.33 mmol), **21ah** was obtained as slightly yellow oil (117 mg, 91%). ¹H NMR (500 MHz, CDCl₃): δ 1.25 (t, *J* = 7.1 Hz, 3H), 1.42 (qd, *J* = 12.3/3.9 Hz, 1H), 1.51–1.61 (m, 3H), 1.71 (dp, *J* = 13.4/3.6 Hz, 1H), 1.89–1.97 (m, 2H), 2.04–2.14 (m, 3H), 2.25–2.33 (m, 2H), 2.53 (tt, *J* = 10.6/3.8

Hz, 1H), 2.72 (d, *J* = 10.8 Hz, 1H), 2.96 (d, *J* = 10.1 Hz, 1H), 4.12 (q, *J* = 7.1 Hz, 2H), 6.03 (d, *J* = 15.8 Hz, 1H), 6.12 (dt, *J* = 15.6/6.7 Hz, 1H), 7.03 (td, *J* = 8.3/2.6 Hz, 1H), 7.12 (dd, *J* = 7.6/1.2 Hz, 1H), 7.18–7.28 (m, 3H), 7.35 (td, *J* = 7.7/1.1 Hz, 1H), 7.58 (d, *J* = 7.5 Hz, 1H) ppm. ¹³C NMR (126 MHz, CDCl₃): δ 14.2, 24.6, 26.3, 27.0, 31.0, 41.8, 53.8, 55.4, 58.1, 60.2, 113.8 (d, ²*J*_{CF} = 20.9 Hz), 116.6 (d, ²*J*_{CF} = 24.5 Hz), 125.1, 126.5, 127.7, 128.2, 130.1, 132.0, 132.5 (d, ³*J*_{CF} = 8.6 Hz), 134.2 (d, ³*J*_{CF} = 10.3 Hz), 136.0 (d, ⁴*J*_{CF} = 3.4 Hz), 136.4, 136.6, 161.7 (d, ¹*J*_{CF} = 249.3 Hz), 174.2 ppm. MS (ESI+) *m/z*: 430 [M + H]⁺. HRMS (EI, 70 eV): M⁺ calcd for C₂₅H₂₉ClFNO₂, 429.1871; found, 429.1875.

1-[(E)-5-(2'-Fluorobiphenyl-2-yl)pent-4-en-1-yl]piperidine-3-carboxylic Acid (13c). According to GP3 from **21c** (79 mg, 0.20 mmol), **13c** was obtained as a slightly yellow solid (63 mg, 86%). ¹H NMR (400 MHz, 0.1 M NaOD/CD₃OD = 1/2, 60 °C): δ 1.37 (qd, *J* = 12.7/4.1 Hz, 1H), 1.52–1.75 (m, 4H), 1.91 (td, *J* = 11.6/2.5 Hz, 1H), 2.02 (m, 2H), 2.11 (q, *J* = 7.1 Hz, 2H), 2.29–2.45 (m, 3H), 2.86 (d, *J* = 10.6 Hz, 1H), 3.11 (d, *J* = 9.8 Hz, 1H), 6.09–6.26 (m, 2H), 7.16–7.23 (m, 2H), 7.23–7.33 (m, 3H), 7.37 (t, *J* = 7.6 Hz, 1H), 7.40–7.48 (m, 1H), 7.61 (d, *J* = 7.9 Hz, 1H) ppm. ¹³C NMR (101 MHz, NaOD/CD₃OD = 1/2, 60 °C): δ 25.8, 26.8, 29.4, 32.0, 46.3, 54.8, 58.2, 59.5, 116.4 (d, ²*J*_{CF} = 22.5 Hz), 125.1 (d, ⁴*J*_{CF} = 3.8 Hz), 126.6, 127.7, 129.1, 129.7, 130.0 (s, ²*J*_{CF} = 16.7 Hz), 130.5 (d, ³*J*_{CF} = 7.9 Hz), 131.3, 132.8, 133.0 (d, ³*J*_{CF} = 3.4 Hz), 135.5, 138.0, 161.0 (d, ¹*J*_{CF} = 244.7 Hz), 182.9 ppm. MS (CI, CH₅⁺) *m/z*: 368 [M + H]⁺. HRMS (EI, 70 eV): M⁺ calcd for C₂₃H₂₆FNO₂, 367.1948; found, 367.1949. Purity: 98.5% (HPLC).

1-[(E)-5-(2',4'-Difluorobiphenyl-2-yl)pent-4-en-1-yl]piperidine-3-carboxylic Acid (13g). According to the GP3, starting from **21g** (83 mg, 0.20 mmol), **13g** was obtained as a slightly yellow solid (68 mg, 88%). ¹H NMR (400 MHz, 0.1 M NaOD/CD₃OD = 1/1, 60 °C): δ 1.25 (qd, *J* = 12.7/4.2 Hz, 1H), 1.35–1.52 (m, 3H), 1.58 (d, *J* = 13.5 Hz, 1H), 1.68 (td, *J* = 11.7/2.3 Hz, 1H), 1.80–1.98 (m, 4H), 2.04–2.14 (m, 1H), 2.14–2.26 (m, 1H), 2.33 (tt, *J* = 12.0/3.8 Hz, 1H), 2.63 (d, *J* = 10.1 Hz, 1H), 2.96 (d, *J* = 11.1 Hz, 1H), 5.90–6.07 (m, 2H), 6.65–6.75 (m, 2H), 6.85–6.95 (m, 2H), 6.99 (t, *J* = 7.5 Hz, 1H), 7.12 (t, *J* = 7.4 Hz, 1H), 7.41 (d, *J* = 7.9 Hz, 1H) ppm. ¹³C NMR (101 MHz, 0.1 M NaOD/CD₃OD = 1/1, 60 °C): δ 25.1, 25.9, 28.7, 31.5, 45.6, 53.6, 57.4, 58.7, 104.4 (d, ²*J*_{CF} = 26.5 Hz), 111.8 (d, ²*J*_{CF} = 21.2, ³*J*_{CF} = 3.5 Hz), 125.4 (dd, ^{2/4}*J*_{CF} = 16.6/3.1 Hz), 126.4, 127.4, 128.6, 129.1, 131.1, 133.1, 133.28 (dd, ^{3/3}*J*_{CF} = 9.5/5.0 Hz), 133.6, 137.3, 160.2 (dd, ^{1/3}*J*_{CF} = 247.2/11.3 Hz), 163.0 (dd, ^{1/3}*J*_{CF} = 247.7/11.4 Hz), 183.4 ppm. MS (CI, CH₅⁺) *m/z*: 386 [M + H]⁺. HRMS (EI, 70 eV): M⁺ calcd for C₂₃H₂₅F₂NO₂, 385.1853; found, 385.1853. Purity: 100% (HPLC).

1-[(E)-5-(2'-Chlorobiphenyl-2-yl)pent-4-en-1-yl]piperidine-3-carboxylic Acid (13p). According to the GP3, starting from **21p** (82 mg, 0.20 mmol), **13p** was obtained as a slightly yellow solid (67 mg, 87%). ¹H NMR (400 MHz, 0.1 M NaOD/CD₃OD = 2/1, 60 °C, MeOH): δ 1.24 (qd, *J* = 12.8/4.2 Hz, 1H), 1.32–1.51 (m, 3H), 1.57 (d, *J* = 13.2 Hz, 1H), 1.66 (td, *J* = 11.5/2.1 Hz, 1H), 1.74–1.98 (m, 4H), 2.00–2.11 (m, 1H), 2.11–2.23 (m, 1H), 2.32 (tt, *J* = 11.5/3.4 Hz, 1H), 2.61 (d, *J* = 10.8 Hz, 1H), 2.94 (d, *J* = 9.6 Hz, 1H), 5.88–5.99 (m, 2H), 6.83 (d, *J* = 7.4 Hz, 1H), 6.89–6.97 (m, 2H), 6.99–7.11 (m, 3H), 7.23 (d, *J* = 7.1 Hz, 1H), 7.39 (d, *J* = 8.2 Hz, 1H) ppm. ¹³C NMR (101 MHz, 0.1 M NaOD/CD₃OD = 2/1, 60 °C, MeOH): δ 25.1, 26.0, 28.7, 31.6, 45.5, 53.6, 57.5, 58.7, 126.1, 127.3, 127.5, 128.7, 128.9, 129.7, 130.1, 130.6, 132.3, 132.7, 133.9, 136.8, 138.3, 140.5, 183.4 ppm. MS (CI, CH₅⁺) *m/z*: 384 [M + H]⁺. HRMS (EI, 70 eV): M⁺ calcd for C₂₃H₂₆ClNO₂, 383.1652; found, 383.1635. Purity: 100% (HPLC).

1-[(E)-5-(2',4'-Dichlorobiphenyl-2-yl)pent-4-en-1-yl]piperidine-3-carboxylic Acid (13z). According to GP3 from **21z** (89 mg, 0.20 mmol), **13z** was obtained as a slightly yellow solid (75 mg, 90%). ¹H NMR (400 MHz, 0.1 M NaOD/CD₃OD = 2/1, 60 °C): δ 1.28 (qd, *J* = 12.4/3.8 Hz, 1H), 1.40–1.54 (m, 3H), 1.60 (d, *J* = 12.8 Hz, 1H), 1.71 (t, *J* = 11.3 Hz, 1H), 1.80–2.01 (m, 4H), 2.04–2.16 (m, 1H), 2.22 (m, 1H), 2.34 (tt, *J* = 11.6/3.6 Hz, 1H), 2.66 (d, *J* = 10.4 Hz, 1H), 2.99 (d, *J* = 10.9 Hz, 1H), 5.88–6.03 (m, 2H), 6.81 (d, *J* = 7.4 Hz, 1H), 6.86 (d, *J* = 8.0 Hz, 1H), 6.93–7.04 (m, 2H), 7.13 (t, *J* =

7.4 Hz, 1H), 7.24 (s, 1H), 7.42 (d, $J = 7.7$ Hz, 1H). ^{13}C NMR (101 MHz, 0.1 M NaOD/ $\text{CD}_3\text{OD} = 2/1$, 60 °C): δ 25.4, 26.3, 28.9, 31.8, 45.7, 54.1, 57.9, 59.0, 126.4, 127.4, 127.7, 128.6, 129.2, 129.8, 130.5, 133.2, 133.3, 134.4, 135.0, 137.1, 137.2, 139.5, 183.1 ppm. MS (CI, CH_3^+) m/z : 418 $[\text{M} + \text{H}]^+$. HRMS (EI, 70 eV): M^+ calcd for $\text{C}_{23}\text{H}_{25}\text{Cl}_2\text{NO}_2$, 417.1262; found, 417.1257. Purity: 99.2% (HPLC).

1-[(E)-5-(2'-Chloro-4'-fluorobiphenyl-2-yl)pent-4-en-1-yl]-piperidine-3-carboxylic Acid (13ah). According to GP3 from **21ah** (86 mg, 0.20 mmol), **13ah** was obtained as a slightly yellow solid (75 mg, 90%). ^1H NMR (400 MHz, NaOD/ $\text{CD}_3\text{OD} = 1/2$, 60 °C): δ 1.36 (qd, $J = 12.6/4.1$ Hz, 1H), 1.51–1.65 (m, 3H), 1.71 (dp, $J = 13.5/3.3$ Hz, 1H), 1.89–2.00 (m, 2H), 2.01–2.13 (m, 3H), 2.27–2.44 (m, 3H), 2.84 (d, $J = 11.0$ Hz, 1H), 3.06 (d, $J = 11.3$ Hz, 1H), 6.00–6.17 (m, 2H), 7.11 (dd, $J = 7.6/1.0$ Hz, 1H), 7.18 (td, $J = 8.4/2.5$ Hz, 1H), 7.21–7.27 (m, 1H), 7.28–7.36 (m, 2H), 7.40 (td, $J = 7.4/1.0$ Hz, 1H), 7.61 (d, $J = 7.3$ Hz, 1H) ppm. ^{13}C NMR (101 MHz, NaOD/ $\text{CD}_3\text{OD} = 1/2$, 60 °C): δ 25.2, 26.0, 28.8, 31.7, 45.7, 54.3, 57.5, 58.9, 115.0 (d, $^2J_{\text{CF}} = 21.3$ Hz), 117.3 (d, $^2J_{\text{CF}} = 25.2$ Hz), 126.4, 127.7, 128.9, 129.3, 130.8, 133.1, 133.6 (d, $^3J_{\text{CF}} = 8.8$ Hz), 134.9 (s, $^3J_{\text{CF}} = 10.2$ Hz), 137.3, 137.5, 137.8, 163.0 (s, $^1J_{\text{CF}} = 248.2$ Hz), 182.9 ppm. MS (ESI+) m/z : 402 $[\text{M} + \text{H}]^+$. HRMS (EI, 70 eV): M^+ calcd for $\text{C}_{23}\text{H}_{25}\text{ClFNO}_2$, 401.1558; found, 401.1558. Purity: 98.0% (HPLC).

Aldehydes. Detailed synthesis protocols for aldehydes are found in the Supporting Information.

MS Binding Experiments. mGAT1 Membrane Preparation. Membrane preparations of HEK293 cells stably expressing mGAT1⁴⁸ were prepared as described previously and stored at –80 °C.^{25,49} On the day of the assay, an aliquot was rapidly thawed and diluted in a 20-fold volume of cold aqueous 0.9% NaCl (m/v). After centrifugation at 15 000 rpm and 4 °C for 20 min (CP56GII, P70AT, Hitachi Ltd., Tokyo, Japan), the pellet was resuspended in ice-cold assay buffer (see below) to a protein concentration of approximately 0.1 mg/mL⁴⁹ as previously described.²⁸

Library Screening. Library screening experiments were performed as reported.²⁸ In short, quadruplicate samples in a total volume of 250 μL were employed. Phosphate buffer, pH 7.1 (12.5 mM $\text{Na}_2\text{HPO}_4 \cdot 2\text{H}_2\text{O}$, 12.5 mM $\text{NaH}_2\text{PO}_4 \cdot \text{H}_2\text{O}$, 1 M NaCl adjusted with 2 M NaOH), was used as incubation buffer. Each sample contained 1% DMSO as final concentration. All solutions were added as 10-fold concentrated stock solutions. Aldehydes were present at 10 μM in the sample, hydrazine **10** at 100 μM . By addition of the mGAT1 membrane preparation, directly after combining hydrazine and aldehydes, a first incubation period of 4 h (for library generation) at 37 °C in a shaking water bath was started. The second incubation period of 40 min was started by addition of the MS marker **6** (20 nM final concentration in the sample). The binding experiment was stopped by a vacuum filtration step (96-well filter plate, Acroprep, glass fiber, 1.0 μm , 350 μL , Pall, Dreieich, Germany, 12-channel pipet). After multiple washing steps with ice-cold aqueous 1 M NaCl, the filter was dried (60 min, 50 °C) and cooled to room temperature. Subsequently the marker was liberated by elution of the filter plate with MeOH into a 96-deep-well plate. Each sample was supplemented with 200 μL of 1 nM [$^2\text{H}_{10}$]NO711 (in MeOH) as internal standard. For calibration, matrix blank samples (produced analogously in absence of NO711) were supplemented with 200 μL of methanolic calibration standards, 50 pM, 100 pM, 500 pM, or 1 nM NO711, and 200 μL of 1 nM [$^2\text{H}_{10}$]NO711 (in MeOH). All samples were dried to completeness (50 °C). For quantification by LC–ESI-MS/MS, samples were reconstituted in 200 μL of 10 mM ammonium formate buffer (pH 7.0)/MeOH (95:5, v/v).

As stated before, each library screening experiment included samples characterizing the pure aldehyde libraries and the pure hydrazine **10**, as well as matrix blanks and zero samples. Total binding and nonspecific binding of NO711 were determined as previously described.²⁸ If the nonspecific binding of the 20 nM NO711 concentration employed was less than 50 pM, the value was extrapolated by linear regression of the nonspecific binding of NO711 concentrations, >20 nM.

By employment of the results obtained for the calibration samples, calibration curves for marker quantitation were generated.

Deconvolution Experiments. The deconvolution experiments were carried out in the same way²⁸ as described for library screening except that the single aldehyde (10 μM per sample) was applied instead of the mixture of four aldehydes.

Competition Experiments Applying Pure Hydrazones. These experiments were performed as recently described,^{25,49} applying the incubation buffer as described for “Library Screening”.

LC–ESI-MS/MS. The methanolic eluates were dried and reconstituted with 10 mM ammonium formate buffer (pH 7.0)/methanol (95:5, v/v). Quantitation by LC–ESI-MS/MS was performed as described utilizing a API 3200 triple-quadrupole mass spectrometer.^{25,49}

Analysis of Binding Experiments. Marker depletion was negligible (<10%) in all binding experiments. Specific binding was defined as the difference between total and nonspecific binding. A nonspecific binding less than 50 pM was not determined experimentally but extrapolated by linear regression for nonspecifically bound NO711 concentrations of ≥ 50 pM. The concentration of a competitor that inhibits 50% of specific binding (IC_{50}) was calculated from competition curves, plotting specifically bound NO711 concentrations vs log competitor concentration (eight different concentrations per competitor) with Prism 4.02 (GraphPad Software, San Diego, CA, U.S.) using the equation for one-site competition and nonlinear curve fitting. Specific binding determined for control samples in the absence of any competitor was set to 100%, whereas the bottom level was set to 0% (corresponds to the nonspecific binding of the employed NO711 concentration). K_i values were calculated according to Cheng and Prussoff⁵⁰ and were expressed as pK_i values. All results are expressed as the mean \pm SEM (unless stated otherwise). pK_i values were determined in at least three separate experiments.

GABA Uptake Assays. [^3H]GABA uptake assays were performed as previously described.⁴⁸

■ ASSOCIATED CONTENT

📄 Supporting Information

General procedures for the synthesis of aldehydes and references and detailed analytic data of aldehydes. This material is available free of charge via the Internet at <http://pubs.acs.org>.

■ AUTHOR INFORMATION

Corresponding Author

*Phone: +49 2180 77249. Fax: +49 2180 77247. E-mail: Klaus.Wanner@cup.uni-muenchen.de.

Present Address

[†]Clinical Trial Oncology, Ente Ospedaliero Ospedali Galliera, Mura delle Cappuccine 14, 16128 Genova, Italy.

Notes

The authors declare no competing financial interest.

■ ACKNOWLEDGMENTS

Special thanks go to Silke Duensing-Kropp and Ljiljana Galogaza for excellent technical support.

■ DEDICATION

Dedicated to Professor H. Zipse with warm wishes on the occasion of his 50th birthday.

■ ABBREVIATIONS USED

BGT, betain γ -aminobutyric acid transporter; CC, column chromatography; DAD, diode array detector; DCC, dynamic combinatorial chemistry; GAT, γ -aminobutyric acid transporter; GP, general procedure; HUGO, human genome organization; IC_{10} , inhibitor concentration that reduces signal to 10%; IC_{20} , inhibitor concentration that reduces signal to

20%; LLOQ, lower limit of quantification; SLC6, solute carrier 6

REFERENCES

- (1) Bowery, N. G.; Smart, T. G. GABA and glycine as neurotransmitters: a brief history. *Br. J. Pharmacol.* **2006**, *147*, S109–S119.
- (2) Beleboni, R. O.; Carolino, R. O. G.; Pizzo, A. B.; Castellán-Baldan, L.; Coutinho-Netto, J.; dos Santos, W. F.; Coimbra, N. C. Pharmacological and biochemical aspects of GABAergic neurotransmission: pathological and neuropsychobiological relationships. *Cell. Mol. Neurobiol.* **2004**, *24*, 707–728.
- (3) Owens, D. F.; Kriegstein, A. R. Is there more to GABA than synaptic inhibition? *Nat. Rev. Neurosci.* **2002**, *3*, 715–727.
- (4) Geffen, Y.; Nudelman, A.; Gil-Ad, I.; Raphaeli, A.; Huang, M.; Savitsky, K.; Klapper, L.; Winkler, I.; Meltzer, H. Y.; Weizman, A. BL-1020: A novel antipsychotic drug with GABAergic activity and low catalepsy is efficacious in a rat model of schizophrenia. *Eur. Neuropsychopharmacol.* **2009**, *19*, 1–13.
- (5) Ishiwari, K.; Mingot, S.; Correa, M.; Trevitt, J. T.; Carlson, B. B.; Salamone, J. D. The GABA uptake inhibitor β -alanine reduces pilocarpine-induced tremor and increases extracellular GABA in substantia nigra pars reticulata as measured by microdialysis. *J. Neurosci. Methods* **2004**, *140*, 39–46.
- (6) Treiman, D. M. GABAergic mechanisms in epilepsy. *Epilepsia* **2001**, *42* (Suppl. 3), 8.
- (7) Aoyagi, T.; Wada, T.; Nagai, M.; Kojima, F.; Harada, S.; Takeuchi, T.; Takahashi, H.; Hirokawa, K.; Tsumita, T. Increased γ -aminobutyrate aminotransferase activity in brain of patients with Alzheimer's disease. *Chem. Pharm. Bull.* **1990**, *38*, 1748–1749.
- (8) Daemen, M. A. R. C.; Hoogland, G.; Cijntje, J.-M.; Spincemaille, G. H. Upregulation of the GABA-transporter GAT-1 in the spinal cord contributes to pain behaviour in experimental neuropathy. *Neurosci. Lett.* **2008**, *444*, 112–115.
- (9) Zádori, D.; Geisz, A.; Vámos, E.; Vécsei, P. K. Valproate ameliorates the survival and the motor performance in a transgenic mouse model of Huntington's disease. *Pharmacol., Biochem. Behav.* **2009**, *94*, 148–153.
- (10) Gajcy, K.; Lochynski, S.; Librowski, T. A role of GABA analogues in the treatment of neurological diseases. *Curr. Med. Chem.* **2010**, *17*, 2338–2347.
- (11) Pilc, A.; Nowak, G. GABAergic hypotheses of anxiety and depression: focus on GABA_B receptors. *Drugs Today* **2005**, *41*, 755–766.
- (12) Krystal, J. H.; Sanacora, G.; Blumberg, H.; Anand, A.; Charney, D. S.; Marek, G.; Epperson, C. N.; Goddard, A.; Mason, G. F. Glutamate and GABA systems as targets for novel antidepressant and mood-stabilizing treatments. *Mol. Psychiatry* **2002**, *7*, S71–S80.
- (13) Kirstensen, A. S.; Andersen, J.; Jørgensen, T. N.; Sørensen, J. E.; Loland, C. J.; Strømgaard, K.; Gether, U. SLC6 neurotransmitter transporters: structure, function, and regulation. *Pharmacol. Rev.* **2011**, *63*, 585–640.
- (14) Madsen, K. K.; Rasmus, P. C.; Larsson, O. M.; Krosgaard-Larsen, P.; Schousboe, A.; White, H. S. Synaptic and extrasynaptic GABA transporters as targets for anti-epileptic drugs. *J. Neurochem.* **2009**, *109*, 139–144.
- (15) Palacín, M.; Estévez, R.; Bertran, J.; Zorzano, A. Molecular biology of mammalian plasma membrane amino acid transporters. *Physiol. Rev.* **1998**, *78*, 969–1054.
- (16) (a) Zhou, Y.; Holmseth, S.; Guo, C.; Hassel, B.; Höfner, G.; Hitfeldt, H. S.; Wanner, K. T.; Danbolt, N. C. Deletion of the γ -aminobutyric acid transporter 2 (GAT2 and SLC6A13) gene in mice leads to changes in liver and brain taurine contents. *J. Biol. Chem.* **2012**, *287*, 35733–35746. (b) Zhou, Y.; Holmseth, S.; Hua, R.; Lehre, A. C.; Olofsson, A. M.; Poblete-Naredo, I.; Kempson, A. A.; Danbolt, N. C. The betaine-GABA transporter (BGT1, slc6a12) is predominantly expressed in the liver and at lower levels in the kidneys and at the brain surface. *Am. J. Physiol.: Renal Physiol.* **2012**, *304*, F316–F328. (c) Lehre, A. C.; Rowley, N. M.; Zhou, Y.; Homseth, S.; Guo, C.; Holen, T.; Hua, R.; Laake, P.; Olofsson, A. M.; Poblete-Naredo, I.; Rusakov, D. A.; Madsen, K. K.; Clausen, R. P.; Schousboe, A.; White, H. S.; Danbolt, N. C. Deletion of the betaine-GABA transporter (BGT1; slc6a12) gene does not affect seizure threshold of adult mice. *Epilepsy Res.* **2011**, *95*, 75–81.
- (17) (a) Iversen, L. L.; Neal, M. J. The uptake of [³H]GABA by slices of rat cerebral cortex. *J. Neurochem.* **1968**, *15*, 1141–1149. (b) Iversen, L. L.; Johnston, G. A. R. GABA uptake in rat central nervous system: comparison of uptake in slices and homogenates and the effects of some inhibitors. *J. Neurochem.* **1971**, *18*, 1939–1950.
- (18) Krosgaard-Larsen, P.; Johnston, G. A. R. Inhibition of GABA uptake in rat brain slices by nipecotic acid, various isoxazoles and related compounds. *J. Neurochem.* **1975**, *25*, 797–802.
- (19) Krosgaard-Larsen, P.; Falch, E.; Larsson, O. M.; Schousboe, A. GABA uptake inhibitors: relevance to antiepileptic drug research. *Epilepsy Res.* **1987**, *1*, 77–93.
- (20) Frey, H.-H.; Popp, C.; Loescher, W. Influence of the inhibitors of high affinity GABA uptake on seizure threshold in mice. *Neuropharmacology* **1979**, *18*, 581–590.
- (21) Ali, F. E.; Bondinell, W. E.; Dandridge, P. A.; Frazee, J. S.; Garvey, E.; Girard, G. R.; Kaiser, C.; Ku, T. W.; Lafferty, J. J.; Moonsammy, G. I.; Oh, H.-J.; Rush, J. A.; Setler, P. E.; Stringer, O. D.; Venslavsky, J. W.; Volpe, B. W.; Yunger, L. M.; Zirkle, C. L. Orally active and potent inhibitors of γ -aminobutyric acid uptake. *J. Med. Chem.* **1985**, *28*, 653–660.
- (22) Dalby, N. O. GABA-level increasing and anticonvulsant effects of three different GABA uptake inhibitors. *Neuropharmacology* **2000**, *39*, 2399–2407.
- (23) Borden, L. A.; Dhar, T. G. M.; Smith, K. E.; Weinsank, R. L.; Branchek, T. A.; Gluchowski, C. Tiagabine, SK& F 89976-A, CI-966, and NNC-711 are selective for the cloned GABA transporter GAT-1. *Eur. J. Pharmacol.* **1994**, *269*, 219–224.
- (24) (a) Andersen, K. E.; Sørensen, J. L.; Huusfeldt, P. O.; Knutsen, L. J. S.; Lau, J.; Lundt, B. F.; Petersen, H.; Suzdak, P. D.; Swedberg, D. B. Synthesis of novel GABA uptake inhibitors. 4.1 Bioisosteric transformation and successive optimization of known GABA uptake inhibitors leading to a series of potent anticonvulsant drug candidates. *J. Med. Chem.* **1999**, *42*, 4281–4291. (b) Andersen, K. E.; Lau, J.; Lundt, B. F.; Petersen, H.; Huusfeldt, P. O.; Suzdak, P. D.; Swedberg, D. B. Synthesis of novel GABA uptake inhibitors. Part 6: Preparation and evaluation of N- Ω asymmetrically substituted nipecotic acid derivatives. *Bioorg. Med. Chem.* **2001**, *9*, 2773–2785.
- (25) Zepperitz, C.; Höfner, G.; Wanner, K. T. MS-binding assays: kinetic, saturation, and competitive experiments based on quantitation of bound marker as exemplified by the GABA transporter mGAT1. *ChemMedChem* **2006**, *1*, 208–217.
- (26) Höfner, G.; Wanner, K. T. Competitive binding assays made easy with a native marker and mass spectrometric quantification. *Angew. Chem., Int. Ed.* **2003**, *42*, S235–S237.
- (27) Höfner, G.; Zepperitz, C.; Wanner, K. T. MS Binding Assays. An Alternative to Radioligand Binding. In *Mass Spectrometry in Medicinal Chemistry*, 1st ed.; Wanner, K. T., Höfner, G., Eds.; Wiley, VCH: Weinheim, Germany, 2007; pp 247–283.
- (28) (a) Sindelar, M.; Wanner, K. T. Library screening by means of mass spectrometry (MS) binding assays—exemplarily demonstrated for a pseudostatic library addressing γ -aminobutyric acid (GABA) transporter 1 (GAT1). *ChemMedChem* **2012**, *7*, 1678–1690. (b) Bucci, M. Methods: how to get GAT. *Nat. Chem. Biol.* **2012**, *8*, 678.
- (29) Kalia, J.; Raines, R. T. Hydrolytic stability of hydrazones and oximes. *Angew. Chem.* **2008**, *47*, 7523–7526.
- (30) Schärer, L.; Smith, J. P. Serum transaminase elevations and other hepatic abnormalities in patients receiving isoniazid. *Ann. Intern. Med.* **1969**, *1113*–1120.
- (31) Huq, F. Molecular modeling analysis of the metabolism of isoniazid. *J. Pharmacol. Toxicol.* **2006**, *1*, 447–455.
- (32) Tafazoli, S.; Mashregi, M.; O'Brien, P. The role of hydrazine in isoniazid-induced hepatotoxicity in a hepatocyte inflammation model. *J. Toxicol. Appl. Pharmacol.* **2008**, *229*, 94–101.

(33) Busch, M.; Dietz, W. Autoxydation der hydrazone. *Ber. Dtsch. Chem. Ges.* **1914**, *47*, 3277–3291.

(34) Harej, M.; Dolec, D. Autoxidation of hydrazones. Some new insights. *J. Org. Chem.* **2007**, *72*, 7214–7221.

(35) Yao, H. C.; Resnick, P. Azo-hydrazone conversion: the autoxydation of benzaldehyde phenylhydrazones. *J. Org. Chem.* **1965**, *30*, 2832–2834.

(36) Miyaura, N.; Yanagi, T.; Suzuki, A. The palladium-catalyzed cross-coupling reaction of phenylboronic acid with haloarenes in the presence of bases. *Chem. Commun.* **1981**, *11*, 513–519.

(37) Andrews, M. D.; Brown, A. D.; Fish, P. V.; Fray, M. J.; Lansdell, M. I.; Ryckmans, T.; Stobie, A.; Vakenhut, F.; Gray, D.; La, F. Preparation of *N*-(Pyrrolidin-3-yl) Carboxamide Derivatives as Serotonin and Noradrenalin Re-Uptake Inhibitors. PCT Int. Appl. WO 2006064351 A2 20060622, 2006.

(38) Kistensen, J.; Lysén, M.; Vedsø, P.; Begrup, M. Synthesis of ortho substituted arylboronic esters by in situ trapping of unstable lithio intermediates. *Org. Lett.* **2001**, *3*, 1435–1437.

(39) Zhao, J.; Yue, D.; Campo, M. A.; Larock, R. C. An aryl to imido-yl palladium migration process involving intramolecular C-H activation. *J. Am. Chem. Soc.* **2007**, *129*, 5288–5295.

(40) Korenaga, T.; Kosaki, T.; Fukumura, R.; Ema, T.; Sakai, T. Suzuki–Miyaura coupling reaction using pentafluorophenylboronic acid. *Org. Lett.* **2005**, *7*, 4915–4917.

(41) Irngartinger, H.; Escher, T. Strong electron acceptor properties of 3'-(pentafluorophenyl)isoxazolol[4',5':1,2][60]fullerene derivatives. *Tetrahedron* **1999**, *55*, 10753–10760.

(42) Zammit, S. C.; Cox, A. J.; Gow, R. M.; Zhang, Y.; Gilbert, R. E.; Krum, H.; Kelly, D. J.; Williams, S. J. Evaluation and optimization of antifibrotic activity of cinnamoyl anthranilates. *Bioorg. Med. Chem. Lett.* **2009**, *19*, 7003–7006.

(43) Wang, Y. D.; Kimball, G.; Prashad, A. S.; Wang, Y. Zr-mediated hydroboration: stereoselective synthesis of vinyl boronic esters. *Tetrahedron Lett.* **2005**, *46*, 8777–8780.

(44) Obtained marker binding of samples of **10** (100 μ M) was in good accordance with published data.

(45) Braestrup, C.; Nielsen, E. B.; Sonnewald, U.; Knutsen, L. J. S.; Andersen, K. E.; Jansen, J. A.; Frederiksen, P. H. A.; Mortensen, A.; Suzdak, P. D. (*R*)-*N*-[4,4-Bis(3-methyl-2-thienyl)but-3-en-1-yl]-nipecotinic acid binds with high affinity to the brain γ -aminobutyric acid uptake carrier. *J. Neurochem.* **1990**, 639–647.

(46) Control experiments confirmed that NMR spectra of the isolated hydrazones before evaporation of the solvent and after resolution with DMSO- d_6 were identical.

(47) 13 C-signal of B–CH was strongly broadened in 13 C NMR spectrum. Chemical shift was determined from cross-peaks of HMQC and HMBC spectra.

(48) Kragler, A.; Höfner, G.; Wanner, K. T. Synthesis and biological evaluation of aminomethylphenol derivatives as inhibitors of the murine GABA transporters mGAT1–GAT4. *Eur. J. Med. Chem.* **2008**, *43*, 2404–2411.

(49) Zepperitz, C.; Höfner, G.; Wanner, K. T. Expanding the scope of MS binding assays to low-affinity markers as exemplified for mGAT1. *Anal. Bioanal. Chem.* **2008**, *391*, 309–316.

(50) Cheng, Y. C.; Prussoff, W. H. Relationship between the inhibition constant (K_i) and the concentration of inhibitor which causes 50 per cent inhibition (IC_{50}) of an enzymatic reaction. *Biochem. Pharmacol.* **1973**, *22*, 3099–3108.